

Synthesis and Reactivity of Aryl- and Alkyl-Rhenium(V) Imido–Triflate Compounds: An Unusual Mechanism for Triflate Substitution

W. Stephen McNeil, Darin D. DuMez, Yoshihiro Matano, Scott Lovell, and James M. Mayer*

Department of Chemistry, University of Washington, Box 351700, Seattle, Washington 98195-1700

Received November 9, 1998

Treatment of the d² rhenium tolylimido complex TpRe(NTol)X₂ with RMgX, RLi, or organozinc reagents yields TpRe(NTol)(R)X [R = Ph, Me, Et, *i*-Pr, *n*-Bu; X = Cl or I; Tol = *p*-tolyl; Tp = hydrotris(1-pyrazolyl)borate] or TpRe(NTol)R₂ (R = Ph, Me). Iodide for triflate metathesis with AgOTf yields TpRe(NTol)(X)OTf [X = Ph, Et, Cl, OTf (=OSO₂CF₃)]. Reaction of TpRe(NTol)(Et)I with excess rather than stoichiometric AgOTf generates the ethylene hydride cation [TpRe(NTol)(η²-C₂H₄)(H)][OTf], which slowly rearranges by ethylene insertion to form TpRe(NTol)(Et)OTf. Treatment of TpRe(NTol)(Ph)I with AgPF₆ gives not iodide abstraction but rather [TpRe(NTol)(Ph)I₂Ag][PF₆], with two Re–I–Ag linkages. Excess pyridine (py) slowly displaces triflate in TpRe(NTol)Ph(OTf) (**11**) to give [TpRe(NTol)Ph(py)][OTf]. The reaction is first-order in **11** and first-order in py. Triflate substitution is similarly slow in the oxo-Tp* derivative, Tp*Re(O)Ph(OTf) [Tp* = HB(3,5-Me₂pz)₃]. These reactions are many orders of magnitude slower than substitution in the oxo-Tp derivative TpRe(O)Ph(OTf). Kinetic and mechanistic data rule out dissociation of triflate ion in or before the rate-determining step and are most consistent with an associative pathway. Reaction with 1,10-phenanthroline gives the κ²-Tp complex [κ²-TpRe(NTol)Ph(phen)][OTf], indicating the lability of one arm of the Tp ligand. TpRe(NTol)Ph₂, TpRe(NTol)Me₂, TpRe(NTol)(Ph)OTf, TpRe(NTol)(OTf)₂, [TpRe(NTol)(Ph)I₂Ag][PF₆], and [κ²-TpRe(NTol)Ph(phen)][OTf] have been structurally characterized. The imido ligand is a better electron donor and has a smaller trans influence than an oxo group in this system.

Introduction

The chemistry of transition metal imido complexes is a vigorous area of study.¹ Such compounds are increasingly used as catalysts or stoichiometric reagents in reactions such as C–H bond activation,² olefin aziridination,³ metathesis,⁴ and ammoxidation.⁵ As one of a series of ligands that form multiple bonds to transition metals, including the isolobal oxo and nitrido groups, imido ligands stabilize high oxidation states and are increasingly of interest for oxidation reactions. The use of rhenium complexes in oxidative processes is also growing.⁶

We have been studying the chemistry of hydrotris(pyrazolyl)borate–rhenium(V)–oxo complexes of the form TpRe(O)X(Y), including various triflate derivatives (X = alkyl, aryl, halide, alkoxide; Y = OTf; Tp = HB(pz)₃).^{7,8} Reaction of these compounds with oxygen atom donors such as pyridine *N*-oxide rapidly generates Re(VII) dioxo complexes, in which intramolecular oxidations of alkyl, aryl, and alkoxide ligands occur.⁸ A recently developed synthesis⁹ has allowed extension of these studies to the related *p*-tolylimido derivatives TpRe(NTol)X(Y), as reported here (Tol = *p*-tolyl). Organometallic imido complexes are not uncommon,¹ including examples with rhenium(V).¹⁰ As in the oxo

(1) (a) Wigley, D. E. *Prog. Inorg. Chem.* **1994**, *42*, 239. (b) Nugent, W. A.; Mayer, J. M. *Metal–Ligand Multiple Bonds*; Wiley-Interscience: New York, 1988.

(2) (a) Schaller, C. P.; Cummins, C. C.; Wolczanski, P. T. *J. Am. Chem. Soc.* **1996**, *118*, 591. (b) Bennett, J. L.; Wolczanski, P. T. *J. Am. Chem. Soc.* **1997**, *119*, 10696. (c) Lee, S. Y.; Bergman, R. G. *J. Am. Chem. Soc.* **1995**, *117*, 5877.

(3) For example: (a) Groves, J. T.; Takahashi, T. *J. Am. Chem. Soc.* **1983**, *105*, 2073–2074. (b) Mansuy, D.; Mahy, J.-P.; Dureault, A.; Bedi, G.; Battioni, P. *J. Chem. Soc., Chem. Commun.* **1984**, 1161. (c) Li, Z.; Quan, R. W.; Jacobsen, E. N. *J. Am. Chem. Soc.* **1995**, *117*, 5889–5890, and references therein.

(4) Alexander, J. B.; La, D. S.; Cefalo, D. R.; Hoveyda, A. H.; Schrock, R. R. *J. Am. Chem. Soc.* **1998**, *120*, 4041–4042, and references therein.

(5) (a) For examples and leading references, see ref 1 and: Reddy, K. L.; Sharpless, K. B. *J. Am. Chem. Soc.* **1998**, *120*, 1207–1217. (b) Chan, D. M.-T.; Fulta, W. C.; Nugent, W. A.; Roe, C.; Tulip, T. H. *J. Am. Chem. Soc.* **1985**, *107*, 251.

(6) (a) Romão, C. C.; Kühn, F. E.; Hermann, W. A. *Chem. Rev.* **1997**, *97*, 3197. (b) Tan, H. S.; Espenson, J. H. *Inorg. Chem.* **1998**, *37*, 467–472, and references therein. (c) Gable, K. P.; Phan, T. N. *J. Am. Chem. Soc.* **1993**, *115*, 3036–3037. (d) Towne, T. B.; McDonald, F. E. *J. Am. Chem. Soc.* **1997**, *119*, 6022–6028. (e) Morimoto, Y.; Iwai, T. *J. Am. Chem. Soc.* **1998**, *120*, 1633–1634. (f) Sinha, S. C.; Sinha, A.; Sinha, S. C.; Keinan, E. *J. Am. Chem. Soc.* **1997**, *119*, 12014–12015.

(7) Abbreviations: Tp, HBpz₃, hydrotris(pyrazolyl)borate; Tp*, HB(3,5-Me₂pz)₃, hydrotris(3,5-dimethylpyrazolyl)borate; Tol, *p*-tolyl; OTf, O₃SCF₃, triflate, or trifluoromethanesulfonate; OTs, O₃SC₆H₄CH₃, tosylate; py, pyridine; pyO, pyridine *N*-oxide; DMSO, Me₂SO, dimethyl sulfoxide.

(8) (a) Brown, S. N.; Mayer, J. M. *J. Am. Chem. Soc.* **1996**, *118*, 12219. (b) DuMez, D. D.; Mayer, J. M. *J. Am. Chem. Soc.* **1996**, *118*, 12416. (c) DuMez, D. D.; Mayer, J. M. *Inorg. Chem.* **1995**, *34*, 6396–6401. (d) *Ibid.* **1998**, *37*, 445–453.

(9) Masui, C.; Mayer, J. M. *Inorg. Chim. Acta* **1996**, *251*, 325.

system, the triflate ligand was introduced as a facile leaving group, as is increasingly common in coordination and organometallic chemistry.^{11,12} The lability of this ligand is due in part to its low basicity and its delocalized charge.¹¹ But the imido–triflate compounds—and the analogous oxo complexes with the more bulky hydrotris(3,5-dimethylpyrazolyl)borate (Tp*)—undergo triflate substitution reactions dramatically slower than the Tp-oxo congeners. The kinetic and mechanistic studies described below indicate an unexpected associative mechanism.

Experimental Section

Experiments were performed under an inert atmosphere using standard vacuum, Schlenk, and glovebox techniques, except where noted. Chromatographic separations were done in the air with silica gel (EM, 200–400 mesh). Protio solvents were degassed and dried according to standard procedures.¹³ Deuterated solvents were purchased from Cambridge Isotope Laboratories, dried over Na (C₆D₆, C₇D₈), P₂O₅ (CD₃CN) or CaH₂ (CD₂Cl₂, CDCl₃), and vacuum transferred immediately prior to use. TpRe(NTol)Cl₂,⁹ TpRe(NTol)I₂,⁹ TpRe(O)Cl(I), TpRe(O)I₂,^{8a} and TpRe(NTol)(Et)Cl⁹ were synthesized according to published procedures. Other reagents were purchased from Aldrich and used as received unless otherwise noted. NEt₃ was degassed and dried over CaH₂, then vacuum transferred prior to use. Pyridine *N*-oxide was sublimed and kept under nitrogen. Me₂SO was degassed and dried over 4 Å molecular sieves. Me₂S was degassed, dried over sodium, and vacuum transferred prior to use. HCl (technical grade) was purchased from Matheson.

NMR spectra were recorded on Bruker AC-200 (¹H, ¹³C, ¹⁹F), DPX-200 (¹H, ¹³C), AF-300 (¹H, ¹³C, ¹³C-DEPT), AM-499, and DRX499 (¹H) Fourier transform spectrometers. All spectra were recorded at ambient temperatures unless otherwise noted. Low-temperature ¹H and ¹³C{¹H} NMR spectra utilized a Bruker B-VT 1000 temperature controller, calibrated by use of the ¹H chemical shifts for methanol.¹⁴ ¹H and ¹³C spectra were referenced to solvent resonances; ¹⁹F spectra to neat CF₃CO₂H. Peak positions are reported in ppm and coupling constants in hertz. The pyrazole protons always have a *J*_{HH} = 2 Hz which is not included in the spectral descriptions below. IR spectra, reported in cm⁻¹, were recorded using a Perkin-Elmer 1600 FT-IR with samples prepared as Nujol mulls or evaporated films on NaCl plates. The pyrazole bands are relatively constant, and therefore the following common bands are not repeated in each of the spectral lists below: 3112 (m), 1498 (m), 1405 (s), 1308 (s), 1209 (s), 1118 (s), 1072 (w), 1049 (vs), 985 (w), 762 (s), 715 (s), 657 (m), 615 (m). Electron impact mass spectra (MS) were recorded using a Kratos Analytical mass spectrometer using a direct probe technique with samples packed into glass capillaries and heated typically to 100 °C.

(10) For examples, see ref 1 and: (a) LaMonica, G.; Cenini, S.; Porta, F. *Inorg. Chim. Acta* **1981**, *48*, 91–95. (b) Chiu, K. W.; Wong, W.-K.; Wilkinson, G.; Galas, A. M. R.; Hursthouse, M. B. *Polyhedron* **1982**, *1*, 31–6; 37–44. (c) Williams, D. S.; Schofield, M. H.; Schrock, R. R. *Organometallics* **1993**, *12*, 4560–4571.

(11) Lawrance, G. A. *Chem. Rev.* **1986**, *86*, 17.

(12) For some recent examples, see: (a) Ferraris, D.; Young, B.; Dudding, T.; Lectka, T. *J. Am. Chem. Soc.* **1998**, *120*, 4548. (b) Howard, W. A.; Bergman, R. G. *Polyhedron* **1998**, *17*, 803. (c) Jaquith, J. B.; Levy, J. C.; Bondar, G. V.; Wang, S. T.; Collins, S. *Organometallics* **1998**, *17*, 914. (d) Chen, J. T.; Chen, Y. K.; Chu, J. B.; Lee, G. H.; Wang, Y. *Organometallics* **1997**, *16*, 1476. (e) Albertin, G.; Antoniutti, S.; Bettiol, M.; Bordignon, E.; Busatto, F. *Organometallics* **1997**, *16*, 4959. (f) Alaimo, P. J.; Arndtsen, B. A.; Bergman, R. G. *J. Am. Chem. Soc.* **1997**, *119*, 2517. (g) Elkin, N.; Dzwiniel, T. L.; Schweibert, K. E.; Stryker, J. M. *Ibid.* **1998**, *120*, 9702–3.

(13) Perrin, D. D.; Armarego, W. L. F. *Purification of Laboratory Chemicals*, 3rd ed.; Pergamon: New York, 1988.

(14) Gordon, A. J.; Ford, R. A. *The Chemist's Companion*; Wiley: New York, 1972; p 303.

Electrospray mass spectra (ESMS) were recorded on a Kratos Profile HV-4 Electrospray MS using MeCN or MeOH as solvent. Elemental analyses were performed by Canadian Microanalytical Services Ltd. (Delta, BC). Some were not made in sufficient quantity to allow elemental analyses to be obtained. In most of these cases, an ¹H NMR spectrum is given in the Supporting Information as proof of bulk purity.

TpRe(NTol)(I)Cl. As an alternative to the previous photochemical procedure,⁹ TpRe(O)Cl(I) (378 mg, 0.654 mmol), excess *p*-toluidine (457 mg, 4.25 mmol, 6.5 equiv), and 350 mL of CH₃CN were refluxed for 4 days under a Dean–Stark trap. After cooling, the solvent was removed to leave a brown residue. The residue was taken up in CH₂Cl₂, filtered, and purified by column chromatography (silica/CH₂Cl₂). The deep green blue band was recovered and recrystallized from methylene chloride/hexanes, yielding 183 mg (42%). Most of the remaining rhenium is recovered as TpRe(NTol)Cl₂ and TpRe(NTol)I₂.

TpRe(NTol)(Ph)Cl (1). PhLi (0.90 mL, 1.8 M in THF, 1.62 mmol) was added to a suspension of ZnCl₂ (68 mg, 0.50 mmol) in THF (5 mL) at –78 °C. While stirring, the mixture was allowed to warm to 0 °C and then transferred into a suspension of TpRe(NTol)Cl₂ (656 mg, 1.00 mmol) in C₆H₆ (100 mL). After stirring for 5 days at room temperature, the solvent was removed under vacuum and the residue was chromatographed (silica/CH₂Cl₂). The teal band was collected and triturated with hexanes to yield **1** as a green powder (223 mg, 36%). Unreacted starting material was also recovered in 26% yield. ¹H NMR (CDCl₃): δ 8.20, 7.81, 7.77, 7.44, 7.29, 7.27 (each d, 1H, pz); 7.09 (dd, 2H, *J*_{HH} = 7, 1 Hz, Ph); 7.29 (t, 2H, *J*_{HH} = 7 Hz, Ph); 7.06, 6.98 (each d, 2H, *J*_{HH} = 8 Hz; NC₆H₄CH₃); 6.85 (tt, 1H, *J*_{HH} = 7, 1 Hz, Ph); 6.43, 6.34, 5.92 (each t, 1H, pz); 2.17 (s, 3H, NC₆H₄CH₃). ¹³C{¹H} NMR (CDCl₃): δ 156.9, 155.2, 144.4, 137.8, 130.4, 126.3, 125.9, 120.1, 147.5, 146.9, 145.6, 138.1, 136.5, 134.0, 107.3, 107.5, 105.6 (pz and aryl carbons); 22.6 (CH₃). IR: 2494 (w, ν_{BH}), 1018 (m), 817 (w), 790 (w). MS: *m/z* = 617 (M⁺). Anal. Calcd for C₂₂H₂₂N₇BClRe: C, 42.83; H, 3.59; N, 15.89. Found: C, 42.61; H, 3.62; N, 15.76.

TpRe(NTol)Ph₂ (2). TpRe(NTol)Cl₂ (1.00 g, 1.74 mmol) was suspended in Et₂O (100 mL). PhMgCl (4.35 mL, 2.0 M in THF, 8.70 mmol, 5 equiv) diluted with 20 mL of Et₂O was added dropwise at room temperature, and the resulting brown mixture was stirred overnight. The green mixture was quenched with 4.0 μL of H₂O, and the solvent was removed in vacuo. The residue was extracted with multiple portions of Et₂O, concentrated, and chromatographed (1:1 toluene/hexanes). The teal band was collected, concentrated under reduced pressure, and recrystallized from THF/hexanes to yield 520 mg (45% yield) of **2** as dark blue-green crystals suitable for X-ray crystallography. ¹H NMR (CD₂Cl₂): δ 7.84, 7.52 (each d, 2H, pz); 7.60, 6.89 (each d, 1H, pz); 7.12 (t, 4H, *J*_{HH} = 7 Hz, Ph); 7.06 (dd, 4H, *J*_{HH} = 7, 1 Hz, Ph); 6.58 (tt, 2H, *J*_{HH} = 7, 1 Hz, Ph); 7.13, 6.86 (each d, 2H, *J*_{HH} = 8 Hz; NC₆H₄CH₃); 6.35 (t, 2H, pz); 6.00 (t, 1H, pz); 2.22 (s, 3H, NC₆H₄CH₃). ¹³C-DEPT (C₆D₆): δ 148.1, 145.9, 142.2, 136.1, 133.8, 130.1, 126.1, 125.8, 121.8, 107.3, 105.5 (pz and aryl carbons); 21.5 (CH₃). IR: 2510 (w, ν_{BH}), 1595 (w), 1568 (w), 1020 (m), 832 (m), 792 (m), 732 (s), 700 (m). MS: *m/z* = 659 (M⁺). Anal. Calcd for C₂₈H₂₇N₇BRRe: C, 51.07; H, 4.13; N, 14.89. Found: C, 51.03; H, 4.18; N, 14.76.

TpRe(NTol)(CH₃)I (3). MeMgCl (3 M in hexanes, 0.04 mL) in 5 mL of Et₂O was slowly added to a –27 °C solution of TpRe(NTol)I₂ (97 mg, 0.128 mmol) in 40 mL of THF. After stirring for 3 h at –27 °C, the mixture was warmed to 10 °C over 4 h. The solution was quenched with 2 mL of water and filtered, and the solvent was removed. The green residue was dissolved in a minimum of toluene and chromatographed (toluene). The deep green band was recrystallized from CH₂Cl₂/hexanes to yield 34 mg of **3** (41%). ¹H NMR (CDCl₃): δ 8.47, 7.75, 7.57, 7.42 (each d, 1H, pz); 7.81 (d, 2H, pz); 7.28, 7.01 (each d, 2H, *J*_{HH} = 8 Hz; NC₆H₄CH₃); 6.42 (t, 2H, pz); 6.00 (t, 1H, pz); 4.82

(s, 3H, ReCH₃); 2.16 (s, 3H, NC₆H₄CH₃). ¹³C{¹H} NMR (CDCl₃): δ 158.8, 149.3, 147.8, 145.4, 137.4, 137.0, 136.4, 133.7, 130.6, 119.9, 107.9, 107.8, 106.2 (pz and aryl carbons); 21.9 (NC₆H₄CH₃); 1.25 (ReCH₃). IR: 2513 (w, ν_{BH}); 1386 (m); 1019 (w); 817 (w); 771 (w); 722 (w). MS: *m/z* = 646 (M+).

TpRe(NTol)(CH₃)₂ (4). MeMgCl (3 M in THF, 0.15 mL) in 10 mL of Et₂O was slowly added to a -40 °C solution of TpRe(NTol)I₂ (209 mg, 0.309 mmol) in 70 mL of THF and stirred for 1 h. The brown mixture was allowed to warm to 15 °C over 15 h, quenched with 2 mL water, and filtered. The green residue was dissolved in a minimum of toluene and chromatographed (toluene). The deep indigo band was collected, concentrated, and recrystallized from CH₂Cl₂/hexanes, yielding 78 mg (47%) of **4**. Crystals suitable for X-ray diffraction were grown by the slow diffusion of pentane into a CH₂Cl₂ solution of **4**. ¹H NMR (C₆D₆): δ 7.83 (d, 2H, pz); 7.48 (d, 1H, pz); 7.35 (d, 2H, pz); 6.92 (d, 1H, pz); 6.92, 6.51 (each d, 2H, J_{HH} = 8 Hz; NC₆H₄CH₃); 5.94 (t, 2H, pz); 5.51 (t, 1H, pz); 5.46 (s, 6H, ReCH₃); 1.69 (s, 3H, NC₆H₄CH₃). ¹³C{¹H} NMR (C₆D₆): δ 157.9, 145.3, 143.2, 136.7, 135.2, 133.5, 130.1, 120.2, 107.6, 105.7 (pz and aryl carbons); 22.1 (NC₆H₄CH₃), 1.1 (ReCH₃). IR: 2485 (w, ν_{BH}); 1367 (m); 1024 (w); 979 (w); 821 (w). MS: *m/z* = 535 (M+). Anal. Calcd for C₁₈H₂₃N₇Br: C, 40.45; H, 4.34; N 18.35. Found: C, 41.46; H, 4.35; N, 18.22.

TpRe(NTol)(Et)I (5). ZnEt₂ (1.0 M in hexanes, 0.31 mL) was added to a benzene (300 mL) solution of TpRe(NTol)I₂ (459 mg, 0.605 mmol) and refluxed under nitrogen for 3 h. The deep green solution was filtered, concentrated, and chromatographed (toluene). The blue-green band was collected, concentrated in vacuo, and recrystallized from CH₂Cl₂/hexanes to yield 363 mg (91%) of **5**. ¹H NMR (CDCl₃): δ 8.35, 7.76, 7.74, 7.67, 7.63, 7.37 (each d, 1H, pz); 5.96 (m, 2H, ReCHHCH₃); 7.20, 6.94 (each d, 2H, J_{HH} = 8 Hz; NC₆H₄CH₃); 6.40, 6.35, 5.96 (each t, 1H, pz); 2.10 (s, 3H, NC₆H₄CH₃); 1.98 (t, 3H, ReCH₂CH₃, J_{HH} = 8 Hz). ¹³C{¹H} NMR (CDCl₃): δ 158.0, 148.3, 146.8, 145.2, 137.4, 137.1, 136.2, 134.0, 130.4, 119.4, 107.5, 107.3, 105.6 (pz and aryl carbons); 28.8 (CH₂CH₃); 22.1, 20.9 (CH₃ groups). IR: 2496 (w, ν_{BH}); 1389 (m); 1014 (w); 814 (w); 767 (w). MS: *m/z* = 660 (M+). Anal. Calcd for C₁₈H₂₂N₇Br: C, 32.74; H, 3.36; N, 14.85. Found: C, 32.79; H, 3.49; N, 14.86.

TpRe(NTol)(*i*-Pr)I (6). Following the preparation of **3**, *i*-PrMgCl (2 M in THF, 0.18 mL) in 10 mL of Et₂O was added to TpRe(NTol)I₂ (242 mg, 0.361 mmol) in 60 mL at -50 °C. Workup as for **5** yielded 146 mg (59%) of green **6**. ¹H NMR (CDCl₃): δ 8.33, 7.88, 7.66, 7.63, 7.52, 7.46 (each d, 1H, pz); 7.80 (sept, 1H, ReCH(CH₃)₂, J_{HH} = 7 Hz); 7.22, 6.95 (each d, 2H, J_{HH} = 8 Hz; NC₆H₄CH₃); 6.35, 6.30, 6.04 (each t, 1H, pz); 2.23, 1.26 (each d, 3H, CH(CH₃)CH₃, J_{HH} = 7 Hz); 1.59 (s, 3H, NC₆H₄CH₃). ¹³C{¹H} NMR (CDCl₃): δ 157.7, 148.8, 147.3, 147.0, 137.2, 137.0, 135.9, 134.4, 130.5, 119.3, 106.7, 106.1, 105.4 (pz and aryl carbons); 39.1 (CH(CH₃)₂); 33.1, 32.6, 22.1 (CH₃ groups). IR: 2498 (w, ν_{BH}); 1391 (m); 1019 (w); 815 (w), 789 (w). MS: *m/z* = 674 (M+). Anal. Calcd for C₁₉H₂₄N₇Br: C, 33.85; H, 3.59; N, 14.55. Found: C, 33.98; H, 3.64; N, 14.53.

TpRe(NTol)(*n*-Bu)I (7). A mixture of *n*-BuLi (2 M in hexanes, 0.28 mL) and ZnCl₂ (74 mg, 0.543 mmol) in 15 mL of Et₂O was slowly added to a benzene (300 mL) solution of TpRe(NTol)I₂ (362 mg, 0.541 mmol) at 5 °C. The mixture turned brown instantly; stirring was continued for an additional 3 h. Chromatography (toluene) resulted in the isolation of 149 mg (40%) of **7** and 22 mg (7%) of a solid spectroscopically identified as TpRe(NTol)(*n*-Bu)Cl. **7**: ¹H NMR (CDCl₃): δ 8.34, 7.80, 7.73, 7.66, 7.61, 7.36 (each d, 1H, pz); 7.18, 6.94 (each d, 2H, J_{HH} = 8 Hz; NC₆H₄CH₃); 7.89, 7.13 (each d of t, 1H, ReCHHCH₂CH₂CH₃, J_{HH} = 4, 7 Hz); 6.38, 6.34, 5.95 (each t, 1H, pz); 2.14 (s, 3H, NC₆H₄CH₃); 1.71, 1.61, 1.50, 1.45 (each m, 1H, ReCH₂CHHCHHCH₂); 0.92 (t, 3H, Re(CH₂)₃CH₃, J_{HH} = 7 Hz). ¹³C{¹H} NMR (CDCl₃): δ 158.3, 147.9, 146.8, 137.3, 137.1, 136.1, 133.9, 130.3, 119.5, 107.6, 107.3, 105.7 (pz and aryl carbons); 46.2 (CH₂(CH₂)₂CH₃); 30.4,

29.8 (CH₂(CH₂)₂CH₃); 23.7, 22.6 (CH₃ groups). IR: 2513 (w, ν_{BH}); 1386 (m); 1019 (w); 820 (w); 788 (w). MS: *m/z* = 688 (M+). Anal. Calcd for C₂₀H₂₆N₇Br: C, 34.90; H, 3.81; N, 14.24. Found: C, 36.79; H, 3.89; N, 14.16.

TpRe(NTol)(*n*-Bu)Cl. ¹H NMR (CDCl₃): δ 7.87, 7.81, 7.74, 7.59, 7.57, 7.39 (each d, 1H, pz); 7.22, 6.96 (each d, 2H, J_{HH} = 8 Hz; NC₆H₄CH₃); 7.79, 7.10 (each d of t, 1H, ReCHHCH₂CH₂CH₃, J_{HH} = 4, 7 Hz); 6.35, 6.33, 5.98 (each t, 1H, pz); 2.13 (s, 3H, NC₆H₄CH₃); 1.73, 1.67, 1.52, 1.46 (each m, 1H, ReCH₂CHHCHHCH₂); 0.94 (t, 3H, Re(CH₂)₃CH₃, J_{HH} = 7 Hz). MS: *m/z* = 597 (M+).

TpRe(NTol)(Ph)I (8). A solution of **2** (594 mg, 0.90 mmol) and I₂ (175 mg, 0.67 mmol, 1.5 equiv) in toluene (50 mL) was refluxed for 2 h. In air, the green solution was washed with aqueous Na₂S₂O₃ and two portions of H₂O, dried over MgSO₄, and filtered. The filtrate was concentrated in vacuo and chromatographed (toluene). Three bands were separated: the initial blue band yielded 68 mg (11%) of unreacted **2**, and the final yellow band afforded a minimal (<5%) amount of TpRe(NTol)I₂. The middle green band was recrystallized from THF/hexanes to yield 515 mg (81%) of **8** as green crystals. ¹H NMR (CD₂Cl₂): δ 8.43, 7.86, 7.80, 7.53, 7.43, 7.22 (each d, 1H, pz); 7.88 (dd, 2H, J_{HH} = 7, 1 Hz, Ph); 7.14 (t, 2H, J_{HH} = 7 Hz, Ph); 7.27, 7.05 (each d, 2H, J_{HH} = 8 Hz; NC₆H₄CH₃); 6.66 (tt, 1H, J_{HH} = 7, 1 Hz, Ph); 6.45, 6.35, 5.99 (each t, 1H, pz); 2.17 (s, 3H, NC₆H₄CH₃). ¹³C-DEPT (C₆D₆): δ 155.6, 150.9, 149.1, 147.8, 146.6, 137.6, 134.1, 131.1, 128.8, 126.6, 120.8, 108.2, 108.3, 106.4 (pz and aryl carbons); 22.2 (CH₃). IR: 2493 (w, ν_{BH}), 1019 (m), 818 (w). MS: *m/z* = 709 (M+). Repeated attempts consistently yielded elemental analyses with low nitrogen values. Anal. Calcd for C₂₂H₂₂N₇Br: C, 37.30; H, 3.13; N, 13.84. Found: C, 37.06; H, 3.43; N, 12.64.

TpRe(NTol)(Ph)Me (9). MeMgCl (0.13 mL, 3.0 M in THF, 0.39 mmol) was added dropwise to a green solution of **8** (230 mg, 0.32 mmol) in toluene (25 mL). The blue solution was quenched with 3 μL of H₂O, reduced to dryness, extracted with Et₂O, and filtered through silica. The blue filtrate was concentrated under reduced pressure and recrystallized from hexane to yield 117 mg (61%) of **9** as blue crystals. ¹H NMR (CDCl₃): δ 7.86, 7.76, 7.74, 7.62, 7.40, 7.02 (each d, 1H, pz); 6.97, 6.74 (each d, 2H, J_{HH} = 8 Hz; NC₆H₄CH₃); 7.19 (t, 2H, J_{HH} = 7 Hz, Ph); 6.96 (dd, 2H, J_{HH} = 7, 1 Hz, Ph); 6.65 (tt, 1H, J_{HH} = 7, 1 Hz, Ph); 6.37, 6.32, 5.87 (each t, 1H, pz); 2.14 (s, 3H, NC₆H₄CH₃); 4.36 (br s, 3H, ReCH₃). ¹³C-DEPT (C₆D₆): δ 146.9, 145.3, 144.2, 143.5, 136.2, 136.0, 133.3, 130.0, 126.1, 125.9, 120.5, 107.4, 107.2, 105.3 (pz and aryl carbons); 21.5, 2.6 (CH₃). IR: 2498 (w, ν_{BH}), 1597 (w), 1567 (w) 1023 (m), 817 (w), 756 (s). MS: *m/z* = 597 (M+). Anal. Calcd for C₂₃H₂₅N₇Br: C, 46.31; H, 4.22; N, 16.44. Found: C, 46.51; H, 4.27; N, 16.49.

TpRe(NTol)Et(OEt) (10). LiOEt (386 mg, 7.42 mmol, 7.5 equiv) was slowly added to a MeCN (120 mL) solution of TpRe(NTol)EtCl (562 mg, 0.989 mmol) and stirred for 4 days, and the solvent was removed under reduced pressure. The residue was extracted with a minimum of benzene and chromatographed (CH₃CN). The blue fraction was immediately dried in vacuo, recrystallized twice from CH₂Cl₂/hexanes, and washed with pentane (3 × 10 mL) to yield 170 mg (29%) of blue **10**. ¹H NMR (C₆D₆): δ 7.93, 7.87, 7.55, 7.39, 7.35, 7.03 (each d, 1H, pz); 7.81, 6.13 (each d of q, 1H, ReCHHCH₃, J_{HH} = 3, 8 Hz); 6.97, 6.60 (each d, 2H, J_{HH} = 8 Hz; NC₆H₄CH₃); 6.00, 5.95, 5.64 (each t, 1H, pz); 5.74, 5.20 (each d of q, 1H, ReOCHHCH₃, J_{HH} = 3, 7 Hz); 2.38 (t, 3H, ReCH₂CH₃, J_{HH} = 7 Hz); 1.79 (s, 3H, NC₆H₄CH₃); 1.75 (t, 3H, ReOCH₂CH₃, J_{HH} = 7 Hz). ¹³C{¹H} NMR (C₆D₆): δ 157.5, 147.0, 145.4, 143.9, 136.8, 135.8, 135.4, 133.6, 129.6, 119.4, 107.0, 106.7, 105.6 (pz and aryl carbons); 82.2 (ReOCH₂CH₃); 28.7 (ReCH₂CH₃); 21.6, 21.3, 19.8 (CH₃ groups). IR: 2507 (w, ν_{BH}); 1367 (m); 1104 (w); 1015 (w); 815 (w); 745 (w). MS: *m/z* = 579 (M+). Anal. Calcd for C₂₀H₂₇N₇BO: C, 41.52; H, 4.71; N, 16.95. Found: C, 41.73; H, 4.72; N, 16.86.

TpRe(NTol)(Ph)OTf (11). AgOTf (212 mg, 0.83 mmol) and **8** (580 mg, 0.82 mmol) were stirred in toluene (50 mL) in the dark at room temperature overnight. The green mixture was filtered, concentrated under reduced pressure, and chromatographed (CH₂Cl₂), a dark green band separating from a light green band. The pale green band contained **13** (<5%, vide infra). Recrystallization from toluene/hexane afforded 507 mg (85%) of **11** as dark green crystals suitable for X-ray diffraction. ¹H NMR (CD₂Cl₂): δ 8.32, 7.88, 7.79, 7.65, 7.21, 7.09 (each d, 1H, pz); 7.32, 7.14 (each d, 2H, J_{HH} = 8 Hz; NC₆H₄CH₃); 7.23 (t, 2H, J_{HH} = 7 Hz, Ph); 6.85 (dd, 2H, J_{HH} = 7, 1 Hz, Ph); 6.81 (tt, 1H, J_{HH} = 7, 1 Hz, Ph); 6.45, 6.38, 6.11 (each t, 1H, pz); 2.28 (s, 3H, NC₆H₄CH₃). ¹³C{¹H} (C₆D₆): δ 156.5, 156.4, 149.0, 148.3, 146.3, 143.8, 139.4, 123.9, 136.3, 134.6, 130.4, 127.7, 126.5, 122.5, 108.2, 107.6, 106.1 (pz and aryl carbons); 21.6 (CH₃). ¹⁹F NMR (CD₂Cl₂): δ -2.03. IR: 2509 (w, ν_{BH}); 1593 (w); 1570 (w); 1336, 1328, 1235, 1181 (s, OTf); 1017 (m); 818 (w); 790 (w); 769 (w); 738 (m); 638 (m); 626 (m). MS: *m/z* = 731 (M⁺). Anal. Calcd for C₂₃H₂₂N₇O₃BF₃SRe·1/2C₇H₈: C, 41.01; H, 3.31; N, 12.63. Found: C, 41.13; H, 3.28; N, 12.56.

TpRe(NTol)(Ph)OTs (12). AgOTs (60 mg, 0.21 mmol) and **8** (140 mg, 0.20 mmol) were sealed in a glass bomb and heated for 72 h at 80 °C in CH₂Cl₂ (15 mL) in the dark. The yellow/green mixture was concentrated *in vacuo*, extracted with THF, filtered, and chromatographed (toluene) to afford 66 mg (44%) of **12** and a trace of TpRe(NTol)(OTs)₂. ¹H NMR (CDCl₃): δ 8.67, 7.77, 7.67, 7.50, 7.14, 7.10 (each d, 1H, pz); 7.72, 7.34, 7.08, 7.04 (each d, 2H, J_{HH} = 8 Hz; C₆H₄CH₃); 7.15 (t, 2H, J_{HH} = 7 Hz, Ph); 6.88 (dd, 2H, J_{HH} = 7, 1 Hz, Ph); 6.78 (tt, 1H, J_{HH} = 7, 1 Hz, Ph); 6.36, 6.32, 5.94 (each t, 1H, pz); 2.31, 2.22 (each s, 3H, C₆H₄CH₃). ¹³C-DEPT (CDCl₃): δ 149.5, 149.0, 146.1, 144.2, 138.2, 136.0, 134.1, 130.2, 129.0, 128.3, 127.3, 127.2, 126.3, 123.0, 107.8, 107.4, 105.8 (pz and aryl carbons); 21.6, 21.0 (CH₃). IR: 2504 (w, ν_{BH}); 1278, 1156 (m, OTs); 1101 (w); 1023 (m); 976 (s); 820 (w); 791 (w); 734 (w); 681 (w). MS: *m/z* = 753 (M⁺). Anal. Calcd for C₂₉H₂₉N₇O₃BSRe·1.1C₇H₈: C, 51.61; H, 4.46; N, 11.48. Found: C, 51.31; H, 4.54; N, 11.41.

TpRe(NTol)(OTf)₂ (13). AgOTf (182 mg, 0.70 mmol, 2.1 equiv), TpRe(NTol)I₂ (256 mg, 0.34 mmol), and toluene (40 mL) were sealed in a glass bomb and heated for 48 h at 85 °C. The green mixture was concentrated under reduced pressure, extracted (3×) with CH₂Cl₂, and filtered. Recrystallization from CH₂Cl₂/hexanes afforded 215 mg (79%) of **13** as green crystals suitable for an X-ray diffraction study. ¹H NMR (CD₂Cl₂): δ 8.02, 7.81 (each d, 2H, pz), 7.93, 7.61 (each d, 1H, pz), 7.54, 7.20 (each d, 2H, J_{HH} = 8 Hz; NC₆H₄CH₃); 6.45 (t, 2H, pz), 6.30 (t, 1H, pz); 2.39 (s, 3H, NC₆H₄CH₃). ¹³C DEPT (CDCl₃): δ 150.0 140.0 139.6 136.2 130.5 124.7 108.5 106.8 (pz and aryl carbons); 21.5 (CH₃). IR: 2517 (w, ν_{BH}), 1592 (w); 1349, 1240, 1189 (m, OTf); 1011 (m); 821 (w). MS: *m/z* = 803 (M⁺). Anal. Calcd for C₁₈H₁₇N₇O₆BF₆S₂Re: C, 26.94; H, 2.14; N, 12.22. Found: C, 26.85; H, 2.17; N, 12.11. ¹⁹F NMR (CD₂Cl₂): δ -1.69.

TpRe(NTol)(Cl)OTf (14). TpRe(NTol)Cl(I) (151 mg, 0.226 mmol) and AgOTf (61 mg, 0.238 mmol, 1.06 equiv) were stirred in CH₂Cl₂ (70 mL) for 3 h. The lime green solution was filtered and concentrated under reduced pressure. The residue was dissolved in methylene chloride, layered with pentane, and allowed to diffuse at -20 °C to afford 124 mg (80%) of **14** as a green powder. ¹H NMR (CD₂Cl₂): δ 7.92, 7.90, 7.85, 7.80, 7.75, 7.58 (each d, 1H, pz); 7.31, 7.16 (each d, 2H, J_{HH} = 8 Hz; NC₆H₄CH₃); 6.51, 6.46, 6.23 (each t, 1H, pz); 2.09 (s, 3H, NC₆H₄CH₃). ¹³C{¹H} NMR (C₆D₆): δ 156.7, 149.0, 148.0, 146.9, 141.2, 138.8, 137.9, 134.7, 130.7, 123.0, 108.7, 108.5, 106.8 (pz and aryl carbons); 21.9 (CH₃). ¹⁹F NMR (C₆D₆): δ -1.10. IR: 2519 (w, ν_{BH}); 1343 (m); 1235 (w, ν_{OTf}); 1018 (w); 819 (w). Anal. Calcd for C₁₇H₁₇N₇BF₃ClO₃SRe: C, 29.64; H, 2.49; N, 14.23. Found: C, 29.89; H, 2.56; N, 14.20.

TpRe(NTol)(Et)OTf (15). AgOTf (138 mg, 0.539 mmol, 1.01 equiv), **5** (351 mg, 0.532 mmol), and CH₂Cl₂ (60 mL) were

stirred for 3 h and then filtered. The solvent was removed *in vacuo*, and the residue was taken up in CH₂Cl₂ and chromatographed on silica/CH₂Cl₂. Recrystallization from CH₂Cl₂/pentane afforded 193 mg of **15** as a dark blue-green solid (54%). ¹H NMR (CD₂Cl₂): δ 8.05, 7.80, 7.75, 7.73, 7.56, 7.44 (each d, 1H, pz); 7.27, 7.09 (each d, 2H, J_{HH} = 8 Hz; NC₆H₄CH₃); 6.30, 5.50 (each d of q, 1H, ReCHHCH₃, J_{HH} = 6, 11 Hz); 6.43, 6.39, 6.18 (each t, 1H, pz); 2.22 (s, 3H, NC₆H₄CH₃); 1.70 (t, 3H, ReCH₂CH₃, J_{HH} = 7 Hz). ¹⁹F NMR (CD₂Cl₂): δ -1.82 ppm. ¹³C{¹H} NMR (CD₂Cl₂): δ 157.2, 148.2, 147.3, 143.7, 140.0, 139.2, 137.0, 135.4, 130.9, 121.2, 108.6, 107.9, 106.6 (pz and aryl carbons); 27.2 (ReCH₂CH₃); 23.4, 23.1 (CH₃ groups). IR: 2515 (w, ν_{BH}), 1594 (w), 1392 (w), 1338 (m, OTf), 1235 (w), 819 (w), 789 (vw), 633 (m). MS: *m/z* = 683 (M⁺).

{[TpRe(NTol)(Ph)I]₂Ag}[PF₆] (16). AgPF₆ (26 mg, 0.102 mmol) and **8** (70 mg, 0.099 mmol) in MeCN (10 mL) were heated at 65 °C in the dark for 18 h, resulting in a green solution with suspended yellow solids. The solution was filtered through Celite and layered with pentane to afford 38 mg (23%) of green prisms suitable for X-ray analysis. ¹H NMR (CD₂Cl₂): δ 8.24, 7.94, 7.86, 7.61, 7.50, 7.24 (each d, 2H, pz); 7.34, 7.16 (each d, 4H, J_{HH} = 8 Hz; NC₆H₄CH₃); 7.28 (t, 4H, J_{HH} = 7 Hz, Ph); 6.79 (dd, 4H, J_{HH} = 7, 1 Hz, Ph); 6.73 (tt, 2H, J_{HH} = 7, 1 Hz, Ph); 6.48, 6.39, 6.09 (each t, 2H, pz); 2.25 (s, 6H, NC₆H₄CH₃). ¹³C DEPT (CD₂Cl₂): δ 148.8, 147.3, 147.0, 139.3, 138.1, 136.8, 135.3, 130.6, 127.7, 126.0, 121.2, 106.9, 106.5, 105.8 (pz and aryl), 21.1 (CH₃). IR: 2535 (w, ν_{BH}), 1591 (m), 1313 (m), 1183 (w), 1051 (s), 1018 (w), 788 (w), 770 (m), 731 (m), 668 (w), 558 (s). ESMS: *m/z* = 1526 (M⁺).

[TpRe(NTol)Ph(NCMe)][OTf] (17). **11** was dissolved in MeCN and heated at 80 °C overnight. In CD₃CN, the conversion is quantitative by NMR. Removal of the solvent affords a tacky green oil. Attempts to crystallize this species or metathesize the ionic triflate anion for other counterions (PF₆⁻, SbF₆⁻, BPh₄⁻, etc.) did not meet with success. ¹H NMR (CD₂Cl₂): δ 8.42, 7.95, 7.91, 7.66, 7.29, 7.05 (each d, 1H, pz); 7.36, 7.17 (each d, 2H, J_{HH} = 8 Hz; NC₆H₄CH₃); 7.26 (t, 2H, J_{HH} = 7 Hz, Ph); 6.98 (d, 2H, J_{HH} = 7 Hz, Ph); 6.97 (tt, 1H, J_{HH} = 7, 1 Hz, Ph); 6.59, 6.44, 6.11 (each t, 1H, pz); 3.47 (s, 3H, NCC₆H₃); 2.17 (s, 3H, NC₆H₄CH₃). ¹³C{¹H} NMR (CD₂Cl₂): δ 155.7, 155.5, 147.0, 146.6, 145.5, 142.9, 139.7, 139.3, 137.6, 136.1, 131.1, 127.4, 127.2, 122.8, 108.9, 108.7, 106.8 (pz and aryl carbons); 22.5 (C₆H₄CH₃); 5.3 (NCCH₃); nitrile carbon not observed. ¹⁹F NMR (CD₂Cl₂): δ -2.92. IR: 3056 (w), 3000 (w), 2926 (w), 2520 (w, ν_{BH}), 2360 (w), 2324 (w), 2285 (w), 2126 (w), 1656 (w), 1592 (m), 1263 (s, OTf), 1159 (s), 1031 (s), 955 (w), 821 (w), 789 (m), 738 (m). Electrospray MS: *m/z* = 623 (M⁺).

[TpRe(NTol)(CH₂CH₂(H))][OTf] (18). AgOTf (9.1 mg, 0.035 mmol, 1.9 equiv), **5** (12.3 mg, 0.019 mmol), and CD₂Cl₂ (0.4 mL) were placed in a sealable NMR tube at -77 °C and warmed to room temperature. The resultant dark brown suspension was spectroscopically characterized. ¹H NMR (CD₂Cl₂): δ 9.40 (d, 1H, ReH, J_{HH} = 3 Hz); 8.65, 8.05, 8.02, 7.93, 7.68, 7.45 (each d, 1H, pz); 7.44, 7.29 (each d, 2H, J_{HH} = 8 Hz; NC₆H₄CH₃); 6.72, 6.49, 6.20 (each t, 1H, pz); 4.64, 4.23, 4.08, 2.58 (each m, 1H, Re(η²-C₂H₄)); 2.45 (s, 3H, Re(NC₆H₄CH₃)). ¹³C{¹H} NMR (CD₂Cl₂): δ 157.2, 150.6, 146.4, 142.8, 138.18, 137.9, 137.6, 131.3, 128.8, 109.3, 109.2, 107.8 (pz and aryl carbons); 23.2 (CH₃); 32.1, 14.4 (C₂H₄).

[TpRe(NTol)Ph(py)]OTf (19). A solution of **11** (33.4 mg, 45.7 μmol) and pyridine (0.20 mL, 2.5 mmol) in dichloromethane was stirred for 2 days at ambient temperature. Evaporation of the solvent resulted in recovery of a green residue, which was triturated with pentane to yield 32 mg of a green powder. All attempts at recrystallization of **19** were unsuccessful, so analytically pure material could not be obtained. Metathesis with NaPF₆ did appear to yield a PF₆⁻ salt, but again recrystallizations were not successful. ¹H NMR (CDCl₃): δ 8.33 (d, 2H, J_{HH} = 5 Hz, pyridine); 7.94, 7.89, 7.78, 7.71, 7.22, 6.88 (each d, 1H, pz); 7.29, 6.77 (each d, 2H, J_{HH} =

8 Hz, NC₆H₄CH₃); 6.81 (t, 1H, $J_{\text{HH}} = 7$ Hz, Ph); 6.56, 6.34, 6.20 (each t, 1H, pz); 2.29 (s, 3H, NC₆H₄CH₃); other pyridine and phenyl resonances obscured. ¹⁹F NMR (CD₂Cl₂): $\delta -2.9$. Electrospray MS: $m/z = 660$ (M⁺).

[κ^2 -TpRe(NTol)Ph(phen)][OTf] (20). A solution of **11** (7.3 mg, 0.010 mmol) and 1,10-phenanthroline (18.0 mg, 0.100 mmol) in C₆D₆ was heated for 3 weeks, resulting in a green solution and green oils. The solvent was removed, and the residue washed with Et₂O. The resulting green powder was redissolved in CH₂Cl₂, and the solution layered with pentane to give small green crystals of **20** suitable for structural analysis. ¹H, ¹³C NMR (HMQC, 499 MHz, CD₂Cl₂): δ 8.80, 141.5; 8.67, 149.0; 8.50, 141.4; 8.43, 129.0; 8.02, 126.5; 7.72, not observed; 7.63, 126.7; 7.45, 149.0 (each dd in ¹H, phen); 8.40 (d, $J_{\text{HH}} = 7$ Hz), 130.7; 8.29 (m), 130.2; 7.01 (t, $J_{\text{HH}} = 7$ Hz), 128.6; 6.79 (t, $J_{\text{HH}} = 7$ Hz), 127.4; 6.41 (tt, $J_{\text{HH}} = 7, 1$ Hz), 139.6 (phenyl); 8.04, 148.6; 7.87, 143.9; 7.82, 138.0; 7.66, 142.3; 7.36, 139.0; 6.14, 143.0 (each d in ¹H, pz); 6.60, 109.3; 6.43, 106.1; 6.02, 108.5 (each t in ¹H, pz); 7.52, 124.0; 7.33, 131.8 each d in ¹H, $J_{\text{HH}} = 8$ Hz, *p*-tol aryl), 2.42, 22.5 (s in ¹H, C₆H₄CH₃). IR: 3450 (br, vs), 2429 (w, ν_{BH}), 1642 (br, s), 1277 (s, OTf), 1260 (s, OTf), 1224 (m), 1157 (m), 1031 (s), 917 (w), 848 (w), 823 (w). Electrospray MS: $m/z = 763$ (M⁺).

Kinetic experiments used 0.5 mL of total solution (deuterated solvent + pyridine), with 10 μ mol of the starting rhenium complex. Reactions were monitored by ¹H NMR spectroscopy using an internal standard, typically hexamethyldisiloxane. Spectra were acquired on a 500 MHz spectrometer using eight scans and a relaxation time long enough to account for the T_1 of the standard. Errors quoted are 2σ values for the best-fit lines of the obtained data.

X-ray Structure Determinations. Data were collected on a Nonius Kappa CCD diffractometer with ω -scans for all complexes except **4**, for which data were collected on an Enraf-Nonius CAD4 diffractometer. KappaCCD data were analyzed (including empirical absorption corrections) using the programs DENZO-SMN, SCALEPACK,¹⁵ and SORTAV.¹⁶ Structure solution for KappaCCD data was carried out by direct methods using SIR92,¹⁷ except for **16**, which was solved by Patterson methods using the program DIRDIF.¹⁸ Structures were refined with SHELXL97,¹⁹ except for **4**, for which SHELXL PC was used.²⁰ All non-hydrogen atoms were refined anisotropically unless otherwise stated. Hydrogen atoms for all structures were refined with a riding model. For **2**, **4**, **11**, **13**, and **20**, hydrogen atoms were placed with idealized geometry and given fixed isotropic displacement parameters of 0.05 (in **20**, the H on B1 was located by difference Fourier synthesis). For **16**, hydrogen atoms were placed with idealized geometry and given fixed isotropic displacement parameters such that they were 1.1 U_{eq} of their parent atom and 1.5 U_{eq} for methyl and water hydrogens. In the structure of **11**, a toluene solvent molecule was found disordered about a 2-fold axis and was refined isotropically. In **20**, disorder in the pendant pyrazole ring was corrected using the DELU and SIMU commands in SHELXL97.¹⁹ Crystallographic data are collected in Table 1, bond lengths and angles in Tables 2–7, and drawings are given in Figures 1–6.

(15) DENZO and SCALEPACK: Otinowski, Z.; Minor, W. In *Methods in Enzymology*; Carter, C. W., Jr., Sweet, R. M., Eds.; Academic Press: New York, 1996; Vol. 276, p 307.

(16) Blessing, R. H. *Acta Crystallogr.* **1995**, *A51*, 33.

(17) Altomare, A.; Cascarano, G.; Giacovazzo, C.; Burla, M. C.; Polidori, G.; Camalli, M. *J. Appl. Crystallogr.* **1994**, *27*, 435.

(18) Beurskens, P. T.; Admirall, G.; Beurskens, G.; Bosman, W. P.; Garcia-Granda, S.; Gould, R. O.; Smits, J. M. M.; Smykalla, C. *DIRDIF*; Crystallography Laboratory, University of Nijmegen: Toerooveld, 6525, ED Nijmegen, The Netherlands.

(19) Sheldrick, G. M. *SHELXL97*; University of Gottingen: Gottingen, Germany, 1998.

(20) Sheldrick, G. M. In *Crystallographic Computing 6*; Flack, P., Parkanyi, P., Simon, K., Eds.; IUCr/Oxford University Press: Oxford, 1993.

Table 1. Crystallographic Data

	2	4	11 ·1/2C ₇ H ₈	13	16 ·H ₂ O	20
empirical formula	C ₂₈ H ₂₇ BN ₇ Re	C ₁₈ H ₂₃ BN ₇ Re	C ₂₃ H ₂₂ BF ₃ N ₇ O ₃ SR _e ·1/2C ₇ H ₈	C ₁₈ H ₁₇ BF ₃ N ₇ O ₃ Re	C ₄₄ H ₄₄ AgB ₂ F ₆ I ₂ N ₁₄ PR _{e2} ·H ₂ O	C ₃₃ H ₃₀ BF ₃ N ₉ O ₃ ReS
<i>M_w</i>	658.58	534.44	776.61	802.52	1687.61	910.75
crystal system	monoclinic	monoclinic	monoclinic	monoclinic	tetragonal	triclinic
space group	P2 ₁ /c	P2 ₁ /n	C2/c	P2 ₁ /n	P4/n	P1
unit cell dimensions (Å, deg)	a = 9.7559(1) b = 27.1769(5) c = 10.3488(2) β = 103.620(1)	a = 12.233(2) b = 18.869(3) c = 18.061(3) β = 102.72(2)	a = 22.6453(3) b = 12.2774(2) c = 24.3021(3) β = 114.844(3)	a = 12.5340(3) b = 14.9950(2) c = 14.6570(3) β = 90.619(3)	a = 18.8489(3) b = 18.8489(3) c = 16.3277(4)	a = 11.841(2) b = 12.644(3) c = 13.1720(17) α = 77.630(13) β = 69.488(11) γ = 83.278(9)
volume (Å ³)	2666.67(8)	4066(1)	6131.31(15)	2754.58(9)	5800.92(19)	1802.2(6)
Z	4	8	8	4	4	2
density (g/cm ³ , calcd)	1.640	1.746	1.683	1.935	1.932	1.678
μ (mm ⁻¹)	4.587	5.994	4.090	4.651	5.654	3.494
λ (Å)	0.71070	0.71070	0.71070	0.71070	0.71070	0.71070
crystal size (mm)	0.47 × 0.38 × 0.19	0.28 × 0.32 × 0.36	0.39 × 0.31 × 0.31	0.31 × 0.25 × 0.16	0.22 × 0.22 × 0.14	0.16 × 0.16 × 0.11
temperature	293	183	161	296	161	161
2 θ range (deg)	2.62–25.32	2.0–50.0	2.95–28.26	2.12–22.20	3.30–29.12	2.12–30.61
index ranges	–9 ≤ h ≤ 9 –29 ≤ k ≤ 29 –12 ≤ l ≤ 12	0 ≤ h ≤ 14 –1 ≤ k ≤ 22 –21 ≤ l ≤ 20	–29 ≤ h ≤ 29 –16 ≤ k ≤ 16 –30 ≤ l ≤ 30	–11 ≤ h ≤ 11 –13 ≤ k ≤ 13 –11 ≤ l ≤ 12	–23 ≤ h ≤ 24 –23 ≤ k ≤ 23 –21 ≤ l ≤ 21	–15 ≤ h ≤ 16 –14 ≤ k ≤ 17 –17 ≤ l ≤ 17
no. of reflns collected	51200	7964	96994	35866	121953	50527
unique reflns	3918	7117	6770	2552	7026	9715
no. of restraints	0	0	0	0	0	3
no. of parameters	334	488	364	370	313	478
final R, R _w (I > 2 σ I)	2.86%, 7.72%	4.70%, 6.34%	3.46%, 9.47%	3.09%, 8.65%	6.70%, 26.30%	8.42%, 19.74%
goodness of fit	1.031	1.03	1.105	0.958	1.085	0.977

Table 2. Selected Bond Lengths (Å) and Angles (deg) in TpRe(N-*p*-tol)Ph₂ (2)

Re-N1	2.222(4)	Re-N7	1.717(4)
Re-N3	2.200(4)	Re-C17	2.149(5)
Re-N5	2.169(4)	Re-C23	2.122(5)
Re-N7-C10	168.2(3)	N1-Re-N7	170.80(16)
C17-Re-C23	92.75(17)	N3-Re-N7	94.47(17)
		N5-Re-N7	106.52(16)

Table 3. Selected Bond Lengths (Å) and Angles (deg) in TpRe(N-*p*-tol)Me₂ (4) (Data for the Two Independent Molecules)

Re-N4	2.267(9), 2.286(7)	Re-N1	1.712(9), 1.698(7)
Re-N2	2.142(8), 2.160(8)	Re-C1	2.140(10), 2.141(10)
R-N6	2.170(7), 2.128(8)	Re-C2	2.139(10), 2.132(12)
Re-N1-C3	174.5(7), 174.6(7)	N1-Re-N4	175.0(3), 176.0(3)
N1-Re-C1	100.6(4), 95.7(4)	N1-Re-N2	99.4(3), 98.6(3)
N1-Re-C2	98.4(4), 99.7(4)	N1-Re-N6	98.2(3), 103.6(3)
C1-Re-C2	87.7(4), 87.4(4)		

Table 4. Selected Bond Lengths (Å) and Angles (deg) in TpRe(N-*p*-tol)(Ph)OTf (11)

Re-N1	2.172(4)	Re-C17	2.120(5)
Re-N3	2.064(4)	Re-O1	2.119(4)
Re-N5	2.189(4)	S1-O1	1.460(4)
Re-N7	1.722(4)	S1-O2	1.388(6)
		S1-O3	1.403(5)
Re-N7-C10	176.9(4)	N1-Re-N7	174.65(17)
C17-Re-O1	83.55(18)	N3-Re-N7	95.88(17)
		N5-Re-N7	95.85(18)

Table 5. Selected Bond Lengths (Å) and Angles (deg) in TpRe(N-*p*-tol)(OTf)₂ (13)

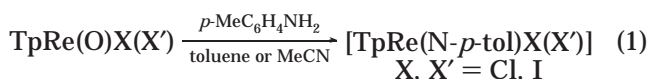
Re-N1	2.157(6)	Re-N7	1.718(6)
Re-N3	2.081(6)	Re-O1	2.081(5)
Re-N5	2.059(7)	Re-O4	2.072(5)
S1-O1	1.441(6)	S2-O4	1.472(6)
S1-O2	1.298(16)	S2-O5	1.426(8)
S1-O3	1.402(15)	S2-O6	1.411(8)
Re-N7-C10	177.9(5)	N1-Re-N7	174.5(3)
O1-Re-O4	81.3(2)	N3-Re-N7	92.4(3)
		N5-Re-N7	97.5(3)

Table 6. Selected Bond Lengths (Å) and Angles (deg) in [TpRe(N-*p*-tol)(Ph)I₂Ag][PF₆] (16)

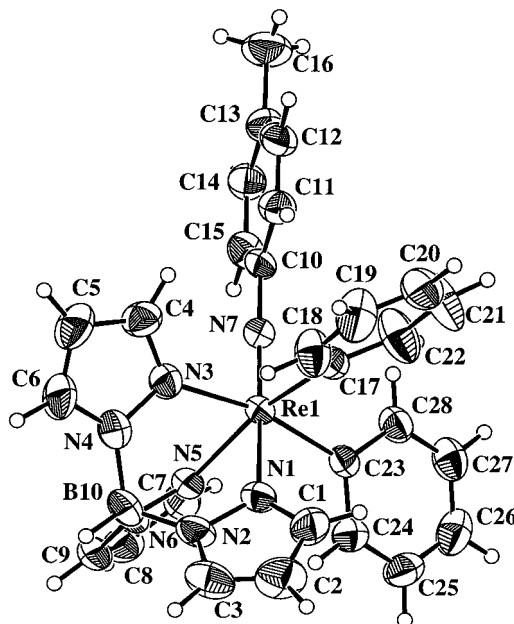
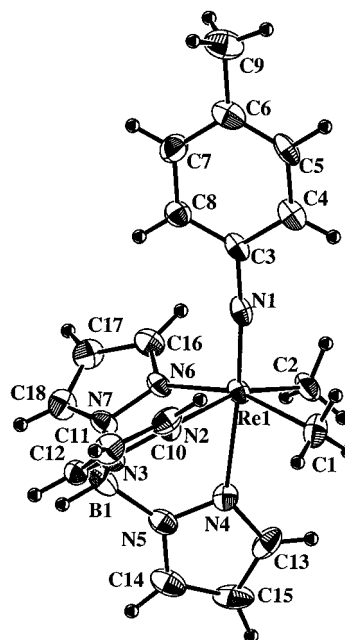
Re-N1	2.197(10)	Re-C17	2.140(12)
Re-N3	2.078(9)	Re-I1	2.7399(11)
Re-N5	2.173(13)	I1-Ag1	2.7916(13)
Re-N7	1.699(12)	Ag1-C22	2.528(13)
Re-N7-C10	176.0(10)	I1-Ag1-I1A	90.2(3)
C17-Re-I1	90.2(3)	C22-Ag1-C22A	131.6(7)
N1-Re-N7	174.5(3)	C22-Ag1-I1	87.6(3)
N3-Re-N7	92.4(3)	C22-Ag1-I1A	115.2(4)
N5-Re-N7	97.5(3)		

Results and Discussion

Syntheses. Reactions of the oxo dihalide complexes TpRe(O)X₂ (X = Cl, I) with *p*-toluidine (CH₃C₆H₄NH₂) in refluxing toluene afford the corresponding imido compounds TpRe(NTol)X₂ in high yields (eq 1).^{7,9} TpRe(O)Cl(I) plus *p*-tolNH₂ in MeCN gives the mixed halide compound TpRe(NTol)Cl(I) with formation of some TpRe(NTol)Cl₂ and TpRe(NTol)I₂. The halide compounds—and all of the neutral complexes reported here—chromatograph well on silica gel in the air, allowing separation of mixtures.

**Table 7. Selected Bond Lengths (Å) and Angles (deg) in [κ²-TpRe(N-*p*-tol)(Ph)(phen)][OTf] (20)**

Re-N3	2.030(9)	Re-N8	2.115(9)
Re-N5	2.128(9)	Re-N9	2.229(9)
Re-N7	1.728(8)	Re-C29	2.124(9)
Re-N7-C22	175.6(7)	N3-Re-N7	98.3(4)
N8-Re-N9	75.9(3)	N5-Re-N7	99.9(3)
N3-Re-N5	90.7(3)	N7-Re-N8	96.2(4)
N7-Re-C29	100.9(4)	N7-Re-N9	171.3(3)

**Figure 1.** ORTEP drawing of TpRe(N-*p*-tol)Ph₂ (2) at the 50% probability level.**Figure 2.** ORTEP drawing of one of the two independent molecules in the structure of TpRe(N-*p*-tol)Me₂ (4) at the 50% probability level.

The imido-dihalide compounds are readily converted into air-stable alkyl and aryl derivatives using Grignard, organolithium, or organozinc reagents (Scheme 1). With the related oxo compounds, Grignard reagents cause decomposition instead of halide metathesis, possibly due

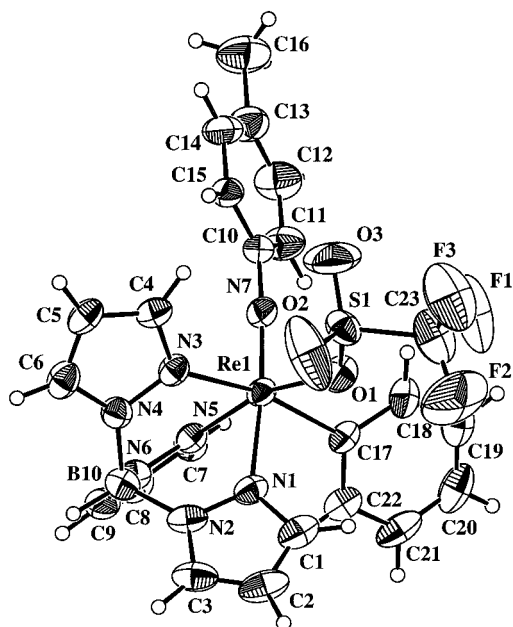


Figure 3. ORTEP drawing of the rhenium complex in $\text{TpRe}(\text{N-}i\text{-p-tol})(\text{Ph})\text{OTf}\cdot\frac{1}{2}\text{C}_7\text{H}_8$ (**11** $\cdot\frac{1}{2}\text{C}_7\text{H}_8$) at the 50% probability level.

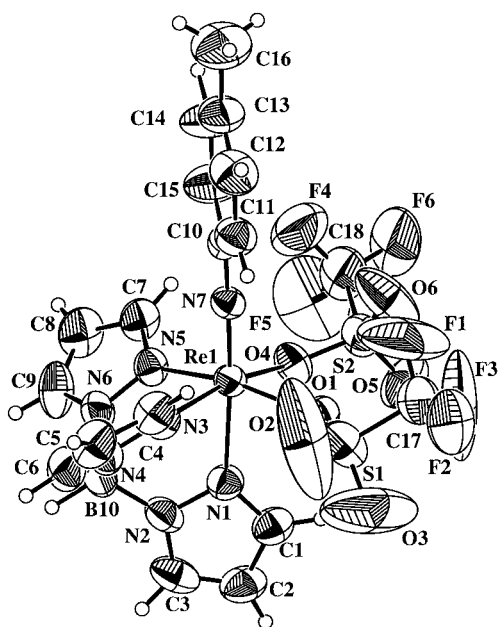


Figure 4. ORTEP drawing of $\text{TpRe}(\text{N-}i\text{-p-tol})(\text{OTf})_2$ (**13**) at the 50% probability level.

to electron-transfer side reactions. The synthetic procedures often reflect the fact that the imido compounds are easier to oxidize (by ca. 0.6 V) and appear to be more difficult to reduce than the oxo complexes.²¹ PhMgCl reacts with $\text{TpRe}(\text{NTol})\text{Cl}_2$ to give the diphenyl complex $\text{TpRe}(\text{NTol})\text{Ph}_2$ (**2**), while "LiZnPh₃" affords only the monophenyl derivative $\text{TpRe}(\text{NTol})(\text{Ph})\text{Cl}$ (**1**) even on prolonged reaction with excess reagent (in contrast to reactions of $\text{TpRe}(\text{O})\text{Cl}_2$ ^{8a}). Reactions with 1 equiv of zinc or magnesium reagents allow the preparation of both monoalkyl compounds $\text{TpRe}(\text{NTol})(\text{R})\text{I}$ ($\text{R} = \text{Me}$ (**3**), Et (**5**), $i\text{-Pr}$ (**6**), $n\text{-Bu}$ (**7**); Scheme 1) typically in 35–65% yields. Since dialkyl complexes are not formed in

(21) Bennett, B. K.; Crevier, T. J.; DuMez, D. D.; Matano, Y.; McNeil, W. S.; Mayer, J. M. submitted.

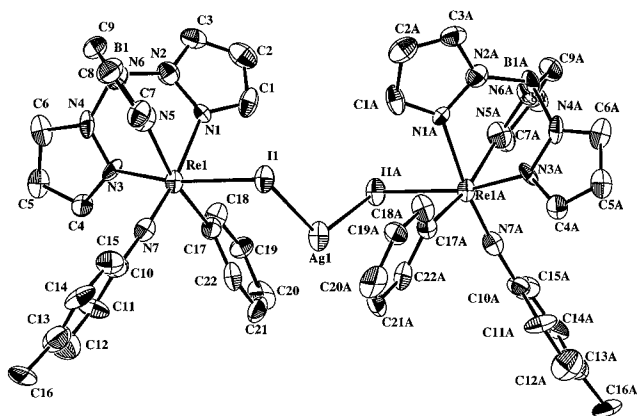


Figure 5. ORTEP drawing of the cation $[\text{TpRe}(\text{N-}i\text{-p-tol})(\text{Ph})\text{I}]_2\text{Ag}[\text{PF}_6]\cdot\text{H}_2\text{O}$ (**16** $\cdot\text{H}_2\text{O}$) at the 50% probability level.

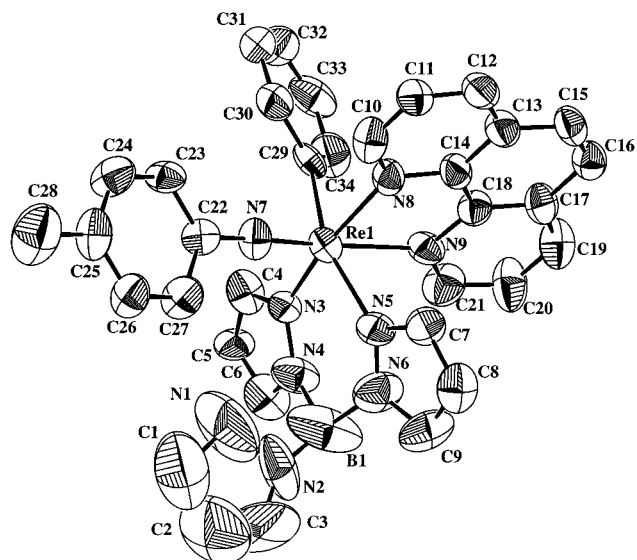
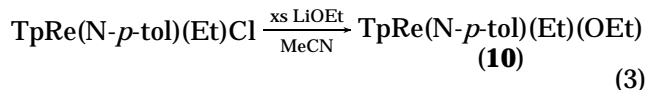
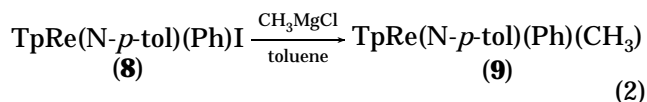
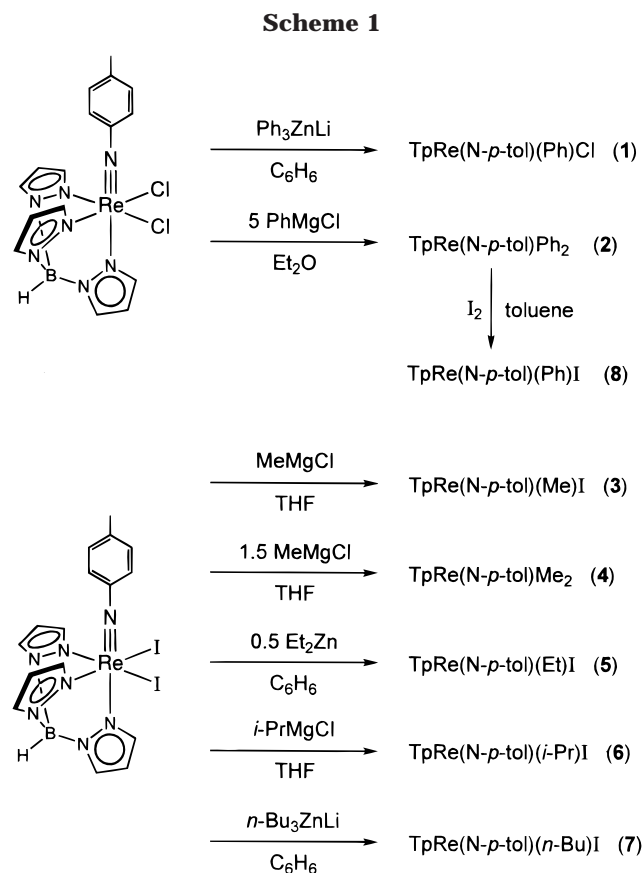


Figure 6. ORTEP drawing of the cation in $[\kappa^2\text{-TpRe}(\text{N-}i\text{-p-tol})(\text{Ph})(\text{phen})][\text{OTf}]$ (**20**) at the 50% probability level.

the $\text{TpRe}(\text{O})$ system,^{8b} an early attempt to prepare the monomethyl derivative used 1.5 equiv of MeMgCl , but this formed a significant amount of the dimethyl complex $\text{TpRe}(\text{NTol})\text{Me}_2$ (**4**). The phenyl iodide complex $\text{TpRe}(\text{NTol})(\text{Ph})\text{I}$ (**8**) is best prepared by treating **2** with I_2 , followed by separation of **2**, **8**, and the diiodide on silica. This is similar to the preparation of $\text{TpRe}(\text{O})(\text{Ph})\text{I}$,^{8a} although milder conditions are needed for the more electron-rich imido complex. Treatment of **8** with MeMgCl affords $\text{TpRe}(\text{NTol})(\text{Ph})\text{Me}$ (**9**) in high yield (eq 2). Reaction of $\text{TpRe}(\text{NTol})\text{Et}(\text{Cl})$ with an excess of LiOEt generates $\text{TpRe}(\text{NTol})\text{Et}(\text{OEt})$ (**10**) (eq 3).

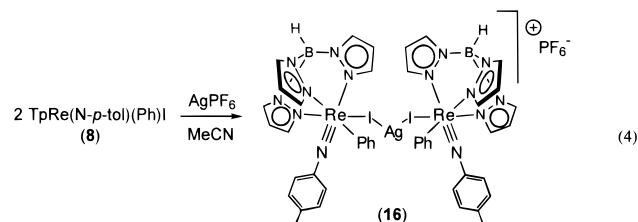


Exchange of iodide ligands for triflate is accomplished with AgOTf in CH_2Cl_2 or toluene (Scheme 2). The phenyltosylate derivative is also accessible from **8** and AgOTf . Some related reactions, such as the treatment of $\text{TpRe}(\text{NTol})(\text{Et})\text{Cl}$ with AgOTf in C_6D_6 , CD_2Cl_2 , or

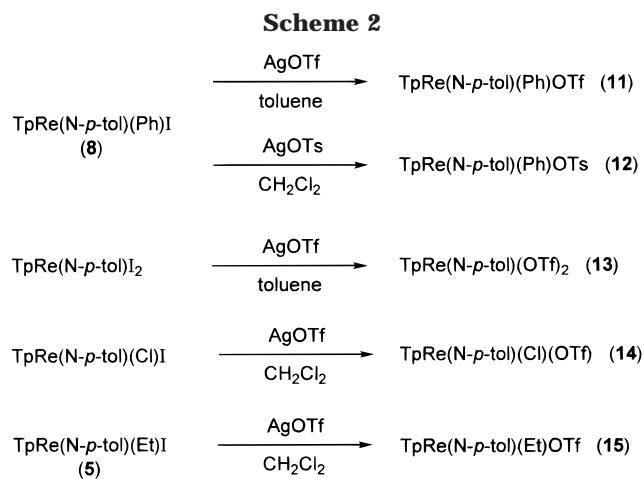


CDCl_3 , proceed instead by electron transfer to give a silver mirror. This is further testament to the electron-richness of the Re(V) imido compounds. The time scales for the AgOTf reactions vary from minutes at room temperature [$\text{TpRe}(\text{NTol})(\text{Et})\text{I}$] to days of heating [$\text{TpRe}(\text{NTol})\text{I}_2$].

In an attempt to introduce PF_6^- as a better leaving group than OTf^- , **8** was reacted with AgPF_6 . Heating overnight at 65 °C gives a green material, **16**, in which the Re–I bonds are still intact (eq 4). The X-ray crystal structure of **16** shows a 2:1 adduct of **8** with Ag^+ , connected via Re–I–Ag linkages: [$\{\text{TpRe}(\text{NTol})(\text{Ph})\text{I}\}_2\text{Ag}\}[\text{PF}_6]$ (Figure 5, Table 6).



The two $\text{TpRe}(\text{NTol})(\text{Ph})\text{I}$ groups are related by symmetry, forming a pinwheel structure about the silver atom. The phenyl ligand is oriented such that the aromatic plane is facing the silver atom, forming a close contact to one of the ortho carbon atoms (Ag–C22, 2.528 (13) Å). Thus, the silver atom is nested in a distorted tetrahedron formed by the iodine and one phenyl carbon atom of each $\text{TpRe}(\text{NTol})(\text{Ph})\text{I}$ fragment. Once formed, **16** is robust, being recovered essentially unchanged after heating at 80 °C in MeCN solution for days. This is surprising since [$\text{TpRe}(\text{NTol})(\text{Ph})(\text{NCMe})$] $^+$ (**17**) is



easily formed on heating the triflate complex **11** in acetonitrile (see below). Similar adducts between transition metal halide compounds and Ag^+ have been crystallographically characterized.²² The related Tp/oxo complex $\text{TpRe}(\text{O})\text{Ph}(\text{I})$ apparently forms an adduct with AgOTf in benzene solution, as observed by NMR and by a color change.²³ In this case, AgI and $\text{TpRe}(\text{O})\text{Ph}(\text{OTf})$ are formed at ambient temperatures so the adduct is not isolable.

Characterization. The $\text{TpRe}(\text{NTol})\text{X}(\text{Y})$ complexes are diamagnetic, octahedral, 18-electron species. NMR spectra indicate the presence of a mirror plane in the symmetric complexes **2**, **4**, and **13**, as expected. The infrared spectra reveal primarily bands due to the Tp ligand, including B–H stretches at ca. 2500 cm^{-1} consistent with κ^3 -coordination.²⁴ Bands at ~ 1020 and $\sim 1360 \text{ cm}^{-1}$ may be due to the Re(NTol) fragment, this assignment often being problematic.¹ Direct inlet mass spectra show parent ions. The covalent nature of the triflate ligands is suggested by the expected mass spectral parent ions, the appropriate bands near 1350 cm^{-1} in the infrared spectra,¹¹ and the fluorine signal in the ^{19}F NMR spectra.^{8,25} The Re(V) imido complexes have vibrant colors ranging from blue-violet to yellow-green. Alkyl and aryl complexes tend toward blue, chloride and sulfonate species tend toward green, and iodide ligands promote a shift toward yellow. The differences are apparently due to shifts in LMCT bands ($\text{I}^- \rightarrow \text{Re}^{\text{V}}$ at lowest energy) rather than changes in the weak $d \rightarrow d$ bands at 750–820 nm.

The crystal structures of diphenyl **2**, dimethyl **4**, phenyl triflate **11**, bis(triflate) **13**, and AgI adduct **16** all show pseudo-octahedral rhenium centers with κ^3 -Tp ligands (Figures 1–5). Crystallographic data are collected in Table 1; selected bond lengths and angles, in Tables 2–6. The imido linkages are all nearly linear, with Re–N–C angles between 168° and 178°. The Re≡NTol distances all fall in the narrow range 1.698(7)–

(22) (a) [$\{\text{CpW}(\text{CO})_3\text{I}\}_4\text{Ag}\}[\text{BF}_4]$: Sal'nikova, T. N.; Andrianov, V. G.; Struchev, Y. T. *Koord. Khim.* **1976**, *2*, 707. (b) For leading references and other examples of M–X–Ag compounds, see: Uson, R.; Fornies, J.; Ara, I.; Casas, J. M. *Polyhedron* **1992**, *11*, 1783. Uson, R.; Fornies, J.; Tomas, M.; Casas, J. M.; Cotton, F. A.; Falvello, L. R. *Inorg. Chem.* **1986**, *25*, 4519.

(23) Brown, S. N. Ph.D. Thesis, University of Washington, 1994; p 116.

(24) Akita, M.; Ohta, K.; Takahashi, Y.; Hikichi, S.; Moro-oka, Y. *Organometallics* **1997**, *16*, 4121.

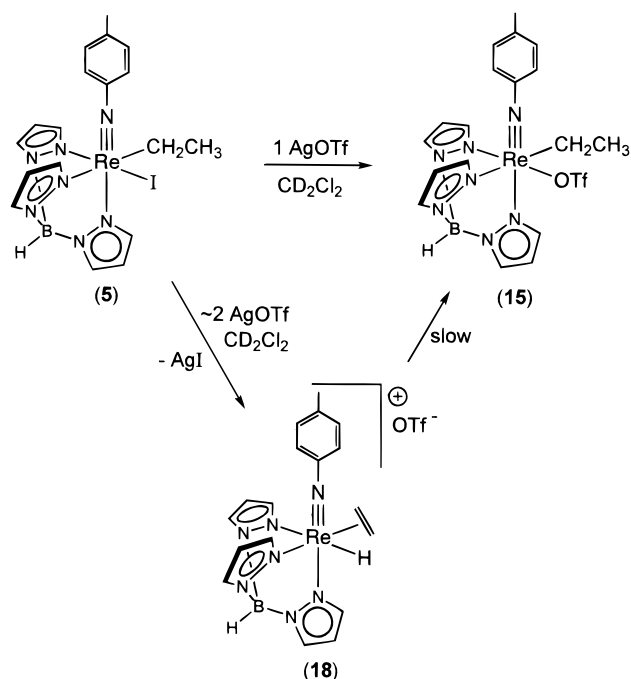
(25) Conry, R. R.; Mayer, J. M. *Organometallics* **1993**, *12*, 3179.

1.718(6) Å, typical of $\text{Re}^{\text{V}}\equiv\text{NR}$ linkages.^{1,9,26} The covalent character of the $\text{Re}-\text{OTf}$ bonds is indicated by the short $\text{Re}-\text{O}$ distances [2.119(4) Å in **11**, 2.077 (av) Å in **13**] and by the longer $\text{S}-\text{ORe}$ bond versus the sulfonyl $\text{S}-\text{O}$ bonds (**11**, 1.460 vs av 1.400; **13**, av 1.457 vs av 1.384). Both these effects are more pronounced in the related oxo compounds: compared to **13**, $\text{TpRe}(\text{O})(\text{OTf})_2$ has shorter $\text{Re}-\text{OTf}$ distances (av, 2.014 Å) and a larger difference in $\text{S}-\text{O}$ bond lengths [1.505 vs 1.400 Å].^{8a} These indicate that the imido complexes are more electron-rich and less Lewis acidic, so the triflate ligands have greater ionic character. These compounds also show a smaller trans-influence for imido versus oxo ligands, as has been observed elsewhere.^{1,27} In $\text{TpRe}(\equiv\text{E})(\text{OTf})_2$, for instance, the difference in $\text{Re}-\text{N}(\text{pz})$ bond lengths trans to the multiple bond versus trans to triflate is 0.087 Å for **13** versus 0.146 Å for the oxo complex.^{8a} The trans influences of imido and phenyl are more comparable, with $\Delta(d_{\text{Re}-\text{N}(\text{pz})}) = 0.038$ Å in **2** and 0.134 Å in $\text{TpRe}(\text{O})\text{Ph}_2$.²⁸ In **11**, the $\text{Re}-\text{N}$ bond trans to phenyl is actually longer than that trans to the imido.

General Reactivity. The alkyl and aryl imido complexes **2–9** are robust species, stable to air in solution for days and as isolated solids indefinitely. Even the triflate, tosylate, and ethoxide complexes **10–15** can be handled in solution under air for short periods and can be purified by column chromatography. This contrasts with the high reactivity of solutions of TpRe -oxo-triflate compounds with air and with silica. The difference is due to the much faster triflate substitutions in the oxo compounds (see below). CH_2Cl_2 solutions of the alkyl-imido compounds are stable to treatment with concentrated aqueous HCl , except for dimethyl **4**, which is consumed instantly. The diphenyl compound **2** reacts cleanly with $\text{H}(\text{OEt})_2\text{BAR}^{\text{F}}_4$ [$\text{Ar}^{\text{F}} = 3,5\text{-C}_6\text{H}_3(\text{CF}_3)_2$] over a few hours in CD_3CN to give benzene and $[\text{TpRe}(\text{NTol})(\text{Ph})(\text{NCCD}_3)][\text{BAR}^{\text{F}}_4]$ (**17** with a $[\text{BAR}^{\text{F}}_4]^-$ counterion).

β -Elimination has not been observed for the alkyl iodide complexes **5–7** or the ethyl-triflate **15**. However, the reaction of **5** with 1.5–2.6 equiv AgOTf gives a new species, identified as the ethylene-hydride complex $[\text{TpRe}(\text{NTol})(\eta^2\text{-C}_2\text{H}_4)(\text{H})][\text{OTf}]$ (**18**) on the basis of ^1H and $^{13}\text{C}\{^1\text{H}\}$ NMR spectra (Scheme 3). The ethylene protons appear as an ABCD pattern (confirmed by decoupling experiments), indicating that ethylene rotation is slow on the NMR time scale at 25 °C. There is a 3 Hz coupling between one of the ethylene protons and the hydride signal at $\delta = 9.40$ ppm, a reasonable chemical shift for a $\text{Re}(\text{V})$ hydride ligand.²⁹ Treatment of **18** with $\text{HCl}(\text{g})$ gives $\text{TpRe}(\text{NTol})\text{Cl}_2$, free ethylene, and H_2 , although not quantitatively. The formation of **18** in ~70% NMR yield from **5** and excess AgOTf is surprising, since 1 equiv of AgOTf gives the ethyl-

Scheme 3



triflate complex **15** in good yield, with only a trace of **18**. A similar pattern is observed on reacting the ethyl-ethoxide **10** with Me_3SiOTf : 0.9 equiv gives **15**, but 2.2 equiv forms **18**. Over a period of hours, solutions of **18** and excess AgOTf convert to **15**, reversing the β -hydrogen elimination. This indicates that **15** is not an intermediate in the formation of **18**. It may be that reactions with excess AgOTf or Me_3SiOTf form an open coordination site and β -hydrogen elimination is faster than triflate coordination under these conditions.

Comparable behavior is observed for isopropyl- and *n*-butyliodide complexes **6** and **7**, but more complicated mixtures are generated. The reaction of **6** with 2.1 equiv of AgOTf in CD_2Cl_2 eventually produces the *n*-propyl complex $\text{TpRe}(\text{NTol})(n\text{-Pr})\text{OTf}$. Isomerization of the propyl ligand is indicated by the appearance of diastereotopic methylene protons of the *n*-propyl group in the ^1H NMR. The *n*-propyl derivative is the expected product of β -hydrogen elimination and reinsertion. Apparently the alkyl complexes are more stable than their alkene-hydride tautomers, and alkene dissociation is not facile. Alkene insertion into $\text{Tp}^*\text{Re}(\text{O})\text{H}(\text{OTf})$ has been reported.²⁹

Substitution Reactions. Substitution of the triflate ligands in $\text{TpRe}(\text{NTol})\text{X}(\text{OTf})$ complexes proceeds slowly, requiring an excess of entering ligand, prolonged reaction times, and/or elevated temperatures. Even at 1 M pyridine (py) concentration, conversion of $\text{TpRe}(\text{NTol})\text{Ph}(\text{OTf})$ (**11**) to $[\text{TpRe}(\text{NTol})\text{Ph}(\text{py})]\text{OTf}$ (**19**) (eq 5) has a half-life of more than 10 h at 21 °C in CD_2Cl_2 . The acetonitrile adduct $[\text{TpRe}(\text{NTol})\text{Ph}(\text{MeCN})]\text{OTf}$ (**17**) is formed from **11** in acetonitrile solution only upon heating. The related rhenium-oxo complex with an hydrotris(3,5-dimethylpyrazolyl)borate ligand, $\text{Tp}^*\text{Re}(\text{O})\text{Ph}(\text{OTf})$,³⁰ also reacts quite slowly with py. These observations contrast with the rapid reactions of the analogous Tp -oxo-triflate $\text{TpRe}(\text{O})\text{Ph}(\text{OTf})$,^{8a} for which

(26) A few recent examples of structurally characterized $\text{Re}(\text{V})$ imido complexes include: (a) Yam, V. W.-W.; Tam, K.-K.; Cheung, K.-K. *J. Chem. Soc., Dalton Trans.* **1995**, 2779. (b) Wittern, U.; Strahle, J.; Abram, U. *Z. Naturforsch. B* **1995**, 50, 597. (c) Luo, H.; Setyawati, I.; Rettig, S. J.; Orvig, C. *Inorg. Chem.* **1995**, 34, 2287. (d) Bakir, M.; Sullivan, B. P. *J. Chem. Soc., Dalton Trans.* **1995**, 1733. (e) Ahmet, M. T.; Coutinho, B.; Dilworth, J. R.; Miller, J. R.; Parrott, S. J.; Zheng, Y. *Polyhedron* **1996**, 15, 2041.

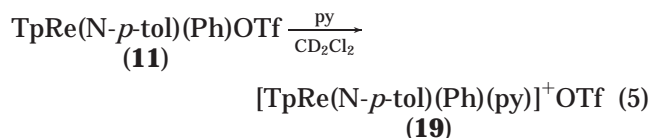
(27) (a) For example, for $\text{TpMo}(\text{E})\text{X}_2$ complexes: Vaughan, W. M.; Abboud, K. A.; Boncella, J. M. *Organometallics* **1995**, 14, 2627.

(28) Brown, S. N.; Myers, A. W.; Fulton, R. J.; Mayer, J. M. *Organometallics* **1998**, 17, 3364–3374.

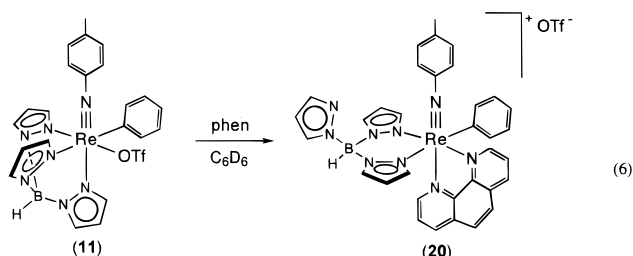
(29) Matano, Y.; Brown, S. N.; Northcutt, T. O.; Mayer, J. M. *Organometallics* **1998**, 17, 2939–2941.

(30) Matano, Y.; Northcutt, T. O.; Bennett, B. K.; Brugman, J.; Mayer, J. M. Manuscript in preparation.

triflate substitution by py, pyO, Me₂S, and Me₂SO all occur within a minute or two at ambient temperatures. At -80 °C, pyO reacts almost within time of mixing and substitution by py is visible within minutes. Other TpRe(O)X(OTf) compounds react similarly.^{8b,c,31} The substitution reactions are easily monitored by ¹H and ¹⁹F NMR spectroscopies, the latter showing a characteristic upfield shift upon changing from covalent to ionic triflate.^{8,25}



Reaction of **11** with 1,10-phenanthroline in C₆D₆ at 80 °C for 3 weeks leads to the formation of [κ²-TpRe-(NTol)Ph(phen)][OTf] (**20**; eq 6). As shown by an X-ray structural study (Figure 6, Table 7), one arm of the Tp ligand is not coordinated in **20**, so that both the Tp and phen ligands are bidentate. The noncoordinated pyrazole exhibits moderate disorder, particularly for the carbon atoms, as indicated by large thermal parameters. The phenanthroline ligand has displaced both the triflate and the pyrazole trans to the imido moiety. The structure of **20** is otherwise unremarkable, with metrical parameters similar to those of related compounds.^{8,9}



The spectroscopic data for **20** are consistent with its solid-state structure. The electrospray mass spectrum exhibits the expected parent peaks centered at *m/z* = 763. The ¹H NMR spectrum is complex in the aromatic region, with signals due to each of the eight phenanthroline protons, five inequivalent phenyl protons, nine pyrazole resonances, and two signals from the tolyl group. The IR spectrum displays bands due to an ionic triflate and a B-H stretching mode at 2429 cm⁻¹. This value is significantly lower than the ~2500 cm⁻¹ observed in the κ³-Tp imido complexes, consistent with the recent report that ν_{BH} is a valuable indicator of Tp hapticity.²⁴

Kinetics of Substitution. Triflate displacement from **11** by excess pyridine in CD₂Cl₂ (eq 5) follows pseudo-first-order kinetics for up to five half-lives, and the resulting rate constants vary linearly with the concentration of pyridine, affording a second-order rate constant of (2.62 ± 0.16) × 10⁻⁵ M⁻¹ s⁻¹ at 21 °C (Figure 7).³² Rate constants over a 60 °C range afford a linear Eyring plot with parameters Δ*H*[‡] = 13.4 ± 0.7 kcal/mol;

(31) The phenoxy triflate complex TpRe(O)OPh(OTf) reacts more slowly with pyridine *N*-oxide than the phenyl complex. There is no reaction at -73 °C, and substitution requires roughly 1 h at -33 °C at typical NMR-tube concentrations.

(32) At concentrations of pyridine above 1.5 M in CD₂Cl₂ (10 mol %), reaction rates become faster than expected, probably due to the increase in solvent polarity.

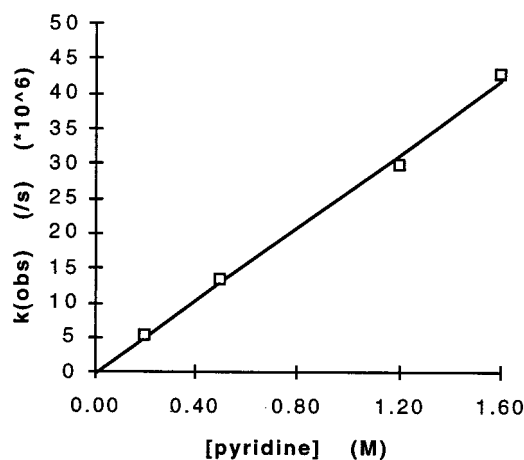


Figure 7. Plot of pseudo-first-order *k*_{obs} vs [py] at 21 °C in CD₂Cl₂ for the reaction of TpRe(N-*p*-tol)Ph(OTf) (**11**) with pyridine (eq 5).

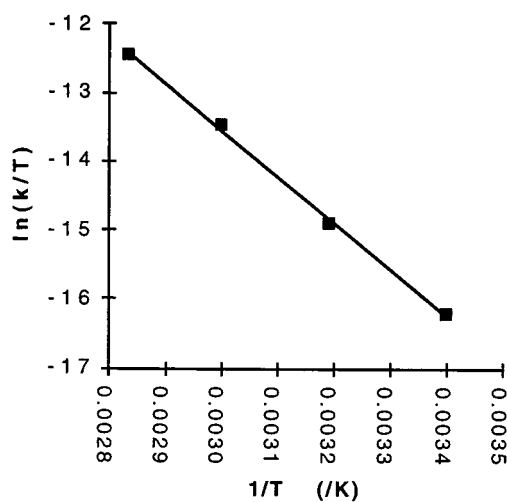


Figure 8. Eyring plot for the reaction of **11** with pyridine (eq 5). *T* = 294, 313, 333, and 353 K.

Δ*S*[‡] = -34 ± 2 eu (Figure 8). Rate constants do not vary appreciably with solvent, with only a 40% increase among C₆D₆ > CD₂Cl₂ ≈ CDCl₃ (Table 8). The dependence on the entering nucleophile is not large: 4-(dimethylamino)pyridine (1.1) > py (1) > pyO (0.6) > *t*-BuNC (0.5) > Me₂SO (0.1) > MeCN (0.03) > 2,6-lutidine (no reaction). It is surprising that the potent nucleophile 4-(dimethylamino)pyridine reacts only 10% faster than pyridine. The lack of reaction of 2,6-lutidine is presumably due to its steric bulk. The nature of the leaving group has a larger effect, as the tosylate derivative TpRe(NTol)Ph(OTs) reacts about 60 times slower than **11**³³ and TpRe(NTol)(Ph)Cl and TpRe(NTol)(Ph)I exhibit no reaction with pyridine. Tp^{*}Re(O)Ph(OTf) also exhibits clean second-order kinetics in its reaction with pyridine, with a rate constant of (4.9 ± 0.4) × 10⁻⁴ M⁻¹ s⁻¹ at 50 °C. This value is 4.6 ± 0.5 times slower than **11** + py under the same conditions.

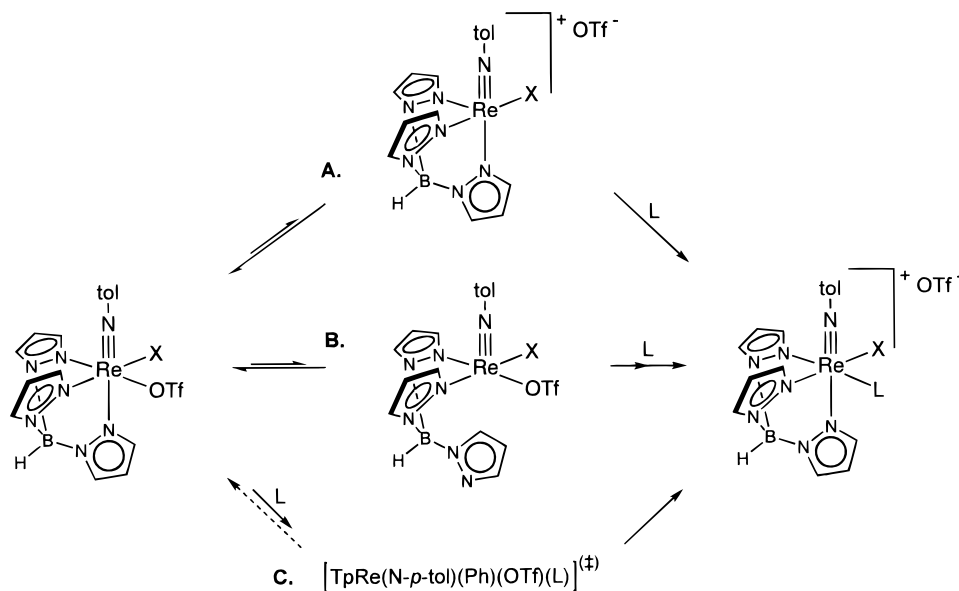
For comparison, triflate substitution by pyridine in the Tp-oxo compound TpRe(O)Ph(OTf) is estimated to occur with a rate constant of ~1 M⁻¹ s⁻¹ at ambient

(33) Prolonged heating of **1** or TpRe(N-*p*-tol)(Ph)(OTs) in methylene chloride, in either the presence or absence of pyridine, produces TpRe(N-*p*-tol)(Ph)Cl, presumably via halide abstraction from the solvent. Although quite slow (*t*_{1/2} ≈ 10 days at 65 °C), this reaction competes with tosylate substitution by py.

Table 8. Second-Order Rate Constants for Substitution Reactions^a

complex	ligand	solvent	temp (°C)	k_2 (M ⁻¹ s ⁻¹)
TpRe(N- <i>p</i> -tol)(Ph)(OTf) (1)	pyridine	CD ₂ Cl ₂	21	$(2.62 \pm 0.16) \times 10^{-5}$
	pyridine	CDCl ₃	21	$(2.39 \pm 0.22) \times 10^{-5}$
	pyridine	C ₆ D ₆	21	$(3.4 \pm 0.5) \times 10^{-5}$
	<i>p</i> -Me ₂ NC ₅ H ₄ N	CD ₂ Cl ₂	21	$(2.91 \pm 0.04) \times 10^{-5}$
	2,6-lutidine	CD ₂ Cl ₂	21	$< 10^{-8}$
	pyridine- <i>N</i> -oxide ^b	CD ₂ Cl ₂	21	$(1.55 \pm 0.17) \times 10^{-5}$
	Me ₂ SO ^b	CD ₂ Cl ₂	21	$(2.64 \pm 0.16) \times 10^{-6}$
	<i>t</i> -BuNC	CD ₂ Cl ₂	21	$(1.29 \pm 0.10) \times 10^{-5}$
	MeCN	CD ₂ Cl ₂	21	$(7.5 \pm 1.5) \times 10^{-7}$
TpRe(N- <i>p</i> -tol)(Ph)(OTs)	pyridine	CD ₂ Cl ₂	56	$(5.47 \pm 0.26) \times 10^{-5}$
	TpRe(N- <i>p</i> -tol)(Ph)(NCMe) ₂][OTf]	pyridine	50	$(5.1 \pm 0.7) \times 10^{-6}$
TpRe(N- <i>p</i> -tol)(Ph)(OTf)	py + 176 mM MeCN	CD ₂ Cl ₂	50	$(5.3 \pm 0.6) \times 10^{-6}$
	py + 335 mM MeCN	CD ₂ Cl ₂	50	$(5.6 \pm 0.5) \times 10^{-6}$
	pyridine	CD ₂ Cl ₂	50	$(4.9 \pm 0.4) \times 10^{-4}$

^a Some k_2 values calculated from experiments with a single ligand concentration, 0.50 M. ^b Rate determined from the disappearance of **1**; the reaction does not give a clean rhenium product.

Scheme 4

temperatures. The imido complex reacts ca. 10^5 times slower than the oxo analogue. It is assumed that the reactions of Tp-oxo compounds also follow second-order kinetics, although this has not been demonstrated. Consistent with second-order substitutions, the related displacement of Me₂SO in [TpRe(O)Ph(OSMe₂)]OTf depends on the nature of the entering ligand, with pyridine reacting much faster than Me₂SO-*d*₆ at low temperatures.

It is not possible to test whether triflate substitution is inhibited by free triflate because of the tight ion pairing in CH₂Cl₂. Such potential inhibition has been tested for the replacement of the acetonitrile ligand in (**17**) by pyridine in CD₂Cl₂ at 50 °C. Adding free MeCN has no discernible affect on the rate (Table 8), so there is no inhibition by the leaving group.

Mechanism of Substitution. Three mechanisms can be readily envisioned for ligand substitution at these rhenium(V) compounds, as illustrated in Scheme 4. We had initially assumed that substitutions would proceed via triflate dissociation, either in a rate-limiting or preequilibrium step (path A). But this pathway is ruled out by the reactions of **11** being slightly faster in benzene-*d*₆ than in the more polar dichloromethane-*d*₂ (dielectric constants $\epsilon = 2.3$ and 8.9, respectively).

Triflate dissociation would involve charge separation and should therefore be faster in more polar solvents. Rate-limiting triflate loss is also inconsistent with the second-order kinetics. Preequilibrium ligand loss is ruled out, at least for substitution of the acetonitrile ligand in **17**, by the lack of inhibition by added MeCN. The observed rate order, Tp-oxo \gg Tp-imido \approx Tp*oxo is opposite that expected given the Re-OTf distances, TpRe(O)(OTf)₂ (2.014 Å av)^{8a} \ll TpRe(N-Tol)(OTf)₂ (2.077 Å av), **11** (2.119 (4) Å) $<$ Tp*Re(O)Ph(OTf) (2.099(5) Å).³⁰ In addition, the increased bulk of the Tp* derivative and the more electron-rich nature of the Tp* and imido derivatives should facilitate dissociation rather than hinder it. The lack of lability cis to the multiple bond in this system is further illustrated by the isolation of the Ag⁺ adduct **16** and its resistance to lose AgI (see above).

The second pathway (B in Scheme 4) involves initial dissociation of the pyrazole trans to the imido or oxo ligand, the pyrazole labilized by the trans influence of the multiply bonded ligand. The isolation of the κ^2 -Tp phenanthroline complex **20** supports the lability of this pyrazole. Rapid preequilibrium pyrazole dissociation followed by rate-limiting ligand addition would show the observed second-order kinetics. The faster reactions of

Tp-oxo compounds would then be due to their larger trans influences versus the Tp-imido complexes.³⁴

The pyrazole-off mechanism, however, does not explain how the entering ligand winds up cis to the multiple bond. Simple trapping of the κ^2 intermediate should give the trans isomer. Pseudorotation of a five-coordinate intermediate could place the open site cis to the multiple bond and triflate trans. This species could then add a ligand in the cis position, with triflate loss and pyrazole recoordination completing the mechanism. But the principle of microscopic reversibility suggests that if a ligand can add to the cis position, it should be able to dissociate from that site as well. The data above show that dissociation cis to the multiple bond is not favorable. While microscopic reversibility only strictly applies to degenerate reactions—in this case, the very slow exchange of the acetonitrile ligand in [TpRe(NTol)-Ph(MeCN)]⁺ with solvent MeCN—it makes this mechanism less attractive. Reversible triflate loss from the five-coordinate κ^2 intermediate is possible though the requirement for two reversible dissociations is similarly unappealing.

We think it more likely that substitution occurs by direct attack of the entering ligand (path C).³⁵ This is consistent with the second-order kinetics and the negative entropy of activation ($\Delta S^\ddagger = -34 \pm 2$ eu). The reactions are slower for the imido versus the oxo derivatives because they are more electron-rich and therefore less Lewis acidic. The Tp*-oxo derivative is both more electron-rich and more sterically hindered than the Tp-oxo analogue. Ligand attack could occur at the Re=E π^* LUMO, which is less accessible for the more electron-rich species. The limited sensitivity to the entering nucleophile and larger dependence on the leaving group suggest an interchange (*I*) description, but the small solvent dependence indicates that anion dissociation is limited at the transition state. An associative (*A*) mechanism is also possible, although the seven-coordinate intermediate would have a 20-electron count since the d² starting materials are all octahedral, 18-electron complexes with Re≡N or Re≡O triple bonds.¹ Formal 20-electron species have been invoked in other substitution reactions,³⁶ including a rhenium-oxo example.³⁷ The 20-electron character could perhaps be avoided by reducing the π -donation from the multiply bonded ligand.

Oxidation Reactions. The impetus for preparing organometallic rhenium(V) imido complexes was to explore oxidation of the organic ligands following oxygen atom transfer to the rhenium center. Reactions of the imido compounds, however, are hampered by the slow triflate substitution. Reactions of ethyl-triflate **15** and pyO in CD₂Cl₂ give small amounts of acetaldehyde and

complex mixtures of rhenium products. To bypass triflate substitution, the ethyl-iodide **5** was treated with AgPF₆ in CD₂Cl₂ in the presence of excess pyO. There is a rapid initial reaction to form acetaldehyde (ca. 20% yield by NMR) and ~10% yield of a new C_s-symmetric rhenium complex, tentatively assigned as TpRe(NTol)-O₂ on the basis of its ¹H NMR spectrum. After the initial period, the liberated pyridine generates the unreactive pyridine adduct [TpRe(NTol)(Et)(py)]⁺. The formation of acetaldehyde and a rhenium(VII) complex is reminiscent of the oxidation of the oxo-ethyl complex TpRe(O)(Et)OTf by excess pyO to give CH₃CHO and TpRe(O)₃ in high yields.^{8b} If the imido complexes follow a similar mechanism—pyO attack at an electrophilic carbene ligand—CH₃CHO and not CH₃CH=NTol would be the expected product.

The phenyl-imido complex TpRe(NTol)Ph(OTf) (**11**) is oxidized by pyO in CD₂Cl₂ over the course of days to give a brown solution. ¹H NMR spectra show free pyridine but no significant concentrations of TpRe complexes. GC-MS analysis of the reaction mixture, either with or without quenching by aqueous HCl, shows the presence of various organic materials including pyridine, pyrazole, and biphenyl. No phenol was observed, although it would have been seen as confirmed by spiking experiments. The imido group does not appear to take part in the oxidation of the organic fragment, as no nitrogen-containing aryl compounds were detected. This messy reaction contrasts with the oxidation of the Tp-oxo analogue TpRe(O)Ph(OTf) by pyO to rhenium-phenoxide and -catecholate products.^{8a} In the imido system, the Re-Ph bond appears to be cleaved with formation of phenyl radicals rather than phenyl migration to an oxo or imido group.

Conclusions

Re(V) imido complexes with alkyl and aryl ligands TpRe(NTol)R(X) have been prepared. Iodide ligands can be exchanged for triflate using AgOTf. Reaction of AgPF₆ with TpRe(NTol)(Ph)I at 65 °C results only in the binding of the iodide to the silver without Re-I cleavage (Figure 5). The imido complexes are more electron-rich and display a smaller trans-influence than the isolobal oxo analogues. Treatment of TpRe(NTol)(Et)I with excess AgOTf—or TpRe(NTol)Et(OEt) with excess Me₃SiOTf—generates an ethylene-hydride complex which slowly forms TpRe(NTol)Et(OTf). Oxidation of TpRe(NTol)Et(OTf) with pyO slowly generates small amounts acetaldehyde, generally mirroring the observed oxo chemistry, although it is less clean. Similar treatment of TpRe(NTol)Ph(OTf) generates a small amount of biphenyl.

Triflate substitution by pyridine and other Lewis bases is quite slow for the rhenium-imido compounds TpRe(NTol)X(OTf) and for the related Tp*-oxo complexes Tp*Re(O)X(OTf). This contrasts with the rapid substitution observed for related Tp-oxo-triflate derivatives. Kinetic and mechanistic experiments show that substitution does not proceed by initial triflate dissociation. In general, loss of a ligand cis to the multiple bond is not facile. Substitution could occur by initial dissociation of the pyrazole trans to the multiply bonded ligand, as suggested by the isolation of a κ^2 -Tp derivative when 1,10-phenanthroline is the entering

(34) Under this argument, the slow reactions of Tp*-oxo complexes would be rationalized by steric inhibition of the second, associative step. The trans influence and Re-N_{trans} distances are comparable in the Tp-oxo and Tp*-oxo complexes.³⁰

(35) (a) Langford, C. H.; Gray, H. B. *Ligand Substitution Processes*; W. A. Benjamin: New York, 1966. (b) Basolo, F.; Pearson, R. G. *Mechanisms of Inorganic Reactions*; Wiley: New York, 1967. (c) Darensbourg, D. J. *Adv. Organomet. Chem.* **1982**, *21*, 113–150.

(36) There are cases of associative substitution reactions proceeding through 20-electron species; for a recent example, see: Holland, P. L.; Andersen, R. A.; Bergman, R. G.; Huang, J.; Nolan, S. P. *J. Am. Chem. Soc.* **1997**, *119*, 12800.

(37) Mayer, J. M.; Tulip, T. H.; Calabrese, J. C.; Valencia, E. *J. Am. Chem. Soc.* **1987**, *109*, 157–163.

ligand. Such a pathway, however, appears to require addition of a ligand *cis* to the multiple bond and is therefore difficult to reconcile with the inertness of *cis* ligands and microscopic reversibility. A mechanism of direct ligand attack at rhenium—interchange or associative—is most consistent with the available data.

Acknowledgment. We are grateful for support from the U.S. National Science Foundation (Grant CHE-9530544 to J.M.M.) and from the National Sciences and Engineering Research Council of Canada for a postdoctoral fellowship to WSM. Y.M. acknowledges a fellow-

ship from the Ministry of Education, Science, Sports, and Culture, Japan. We thank Drs. David Barnhart and Martin Salidek for their assistance with X-ray crystallographic and mass spectrometric experiments, Professor Seth Brown for valuable discussions, and Aaron Meldahl and Jake Soper for their assistance.

Supporting Information Available: Data from X-ray crystal structures of complexes **2**, **4**, **11**, **13**, **16**, and **20** and ¹H NMR spectra of **3**, **4**, **7**, **15**, **16**, **19**, and **20**. This material is available free of charge via the Internet at <http://pubs.acs.org>.

OM980914I